Time-Resolved Protein Fluorescence

The previous chapter described the general features of intrinsic protein fluorescence. We described the spectral properties of the aromatic amino acids and how these properties are influenced by the surrounding protein structure. We now describe time-resolved measurements of protein fluorescence. Such measurements have become increasingly common because of the increased availability of time-domain (TD) and frequency-domain (FD) instrumentation.[1,2] However, time-resolved studies of intrinsic protein fluorescence are made challenging by the lack of simple pulsed light sources. Pulsed laser diodes are not yet available for excitation of protein fluorescence. Pulsed LEDs for excitation of protein fluorescence have just been announced, but the pulse widths are over one nanosecond. Single-photon excitation of protein fluorescence requires wavelengths in the range from 280 to 305 nm. Prior to about 2000, the dominant pulsed light source for this range of wavelengths was a synchronously pumped cavity-dumped dye laser, typically rhodamine 6G, which was doubled to obtain the UV wavelengths. The synchronously pumped dye lasers require an actively mode-locked pump laser, typically an argon ion or Nd:YAG laser. At present the actively mode-locked lasers are becoming less available because of the widespread use of Ti:sapphire lasers. These lasers spontaneously mode lock and may not use an active mode locker. Wavelengths suitable for excitation of protein fluorescence can be obtained by frequency tripling the long-wavelength output of a Ti:sapphire laser. Tripling the output at 840 nm yields 280 nm. The femtosecond pulse widths from Ti:sapphire lasers make it practical to generate such harmonics. Excitation of intrinsic protein fluorescence can also be accomplished with synchrotron radiation. Many of the recent studies of time-resolved intrinsic protein fluorescence used the frequency-tripled output of a pulsed Ti:sapphire laser or synchrotron radiation.

Even with the best available instrumentation it is challenging to interpret the time-dependent data from proteins. The intensity decays of proteins are usually complex and often depend on observation wavelength. The complexity is due to both the presence of multiple-tryptophan residues in a single protein and the complex decay kinetics displayed by even single-tryptophan residues in proteins. High time resolution and high signal-to-noise measurements are needed to resolve the multiple components in these decays. Once the multi-exponential intensity decays are resolved, it is tempting to assign the various components to the individual tryptophan residues in multi-tryptophan proteins. However, even proteins with a single tryptophan residue typically display two or more decay times.[3,4] Hence, there is no reason to believe that the individual decay times represent individual trp residues, until this fact is demonstrated by additional experiments. In some cases, where the decay times are very different, it has been possible to assign decay times to individual tryptophan residues. This assignment typically relies on the use of mutant proteins containing one tryptophan or a fewer number of tryptophans than are present in the wild-type protein.

An additional complication is that tryptophan itself in solution at neutral pH displays a multi-exponential or non-exponential decay. The heterogeneity is moderately weak. Most of the emission from tryptophan occurs with a decay time near 3.1 ns. There is also a second component with a decay time near 0.5 ns. For some time the origin of this component was not known. It appears that most of heterogeneity of the tryptophan decay is due to the presence of conformational isomers, called rotamers, which display distinct decay times. However, there may be additional factors that contribute to the complex decay kinetics of tryptophan.

Interpretation of the intensity decays becomes more complicated because of additional processes that may not occur for the isolated amino acids. Energy transfer can occur from tyrosine to tryptophan, or between tryptophan residues themselves. Following excitation the tryptophan emission can display time-dependent spectral shifts due to

relaxation of the solvent or the protein matrix around the excited-state dipole moment. Proteins may exist in several conformations, each of which displays different intensity decay. Another source of complexity is the possibility of transient effects in collisional quenching, due to either added quenchers or the presence of nearby quenching groups in the protein. In principle, all these phenomena can be studied using time-resolved measurements. In practice, it is difficult to determine the contributions of each phenomenon to the intensity decay. The use of engineered proteins is critical to resolving these complex interactions.

While the interpretation of time-resolved protein fluorescence is not always simple, the time-resolved data provide opportunities for a more detailed understanding of protein structure and function. In favorable cases it is possible to resolve the emission spectra of individual tryptophan residues based on the time-dependent decays measured at various emission wavelengths. The time-resolved decays can sometimes be interpreted in terms of the location of the tryptophan residues in proteins, and the interactions of these residues with nearby amino-acid residues in the protein. Conformation changes in proteins often result in changes in the intensity decay due to altered interactions with nearby groups. The time-dependent anisotropy decays are invariably informative about the extent of local protein flexibility and the interactions of a protein with other macromolecules. Also, fluorescence quenching is best studied by time-resolved measurements, which can distinguish between static and dynamic processes. And, finally, it is now known that proteins can be phosphorescent at room temperature. The phosphorescence decay times are sensitive to exposure to the aqueous phase as well as the presence of nearby quenchers. In this chapter we present an overview of time-resolved protein fluorescence, with examples that illustrate the range of behavior seen in proteins.

17.1. INTENSITY DECAYS OF TRYPTOPHAN: THE ROTAMER MODEL

One difficulty in interpreting the time-resolved intensity decays of proteins has been a lack of understanding of the intensity decay of tryptophan itself. In neutral aqueous solution the intensity decay of tryptophan is known to be a double exponential, with decay times near 3.1 and 0.5 ns (Table 17.1).[4–12] The dominant origin of a bi-exponential decay of tryptophan is the presence of rotational isomers (Figure 17.1). In solution the side chain of tryptophan can adopt various conformational states, which appear to interchange slowly on the ns timescale. A tryptophan solution can be regarded as a mixture of these rotational isomers, called rotamers. In neutral aqueous solution, tryptophan is present in the zwitterionic form in which the amino group

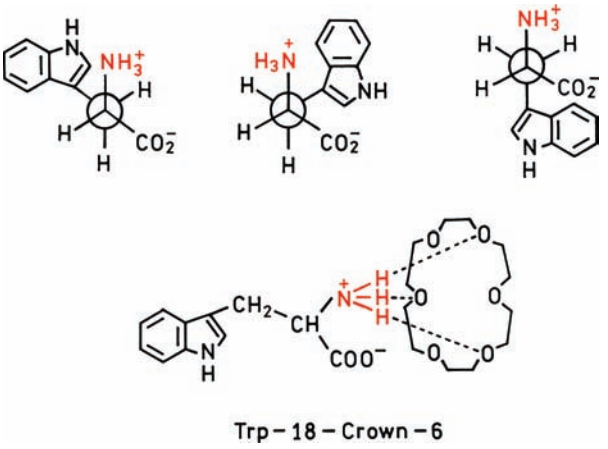

Figure 17.1. Rotational isomers of tryptophan rotamers. The rotamers on the left is thought to be responsible for the 0.5-ns decay time. The lower section shows tryptophan complexed with 18-Crown-6, which prevents quenching by the ammonium group. Revised from [12,27].

Table 17.1. Intensity Decays of the Aromatic Amino Acids and Related Compounds at 20°C, pH 7

Compound	τ_1 (ns)	τ_2 (ns)	α_1	α_2	λ_{em} (nm)	Ref.
Indole	4.4	–	1.0	–	350	–
Tryptophan	3.1	0.53	0.67	0.33	330	6
NATA	3.0	–	1.0	–	330	6
Phenol	3.16	–	1.0	–	300	32, 34
Tyrosine (pH 6)	3.27	–	1.0	–	300	32, 34
Tyrosine (pH 5.5)	3.40	0.98	0.41	0.58	350	43
O-Methyl tyrosine (pH 5.5)	4.84	–	1.0	–	310	34
NATyrA	1.66	0.11	0.65	0.35	300	32, 34

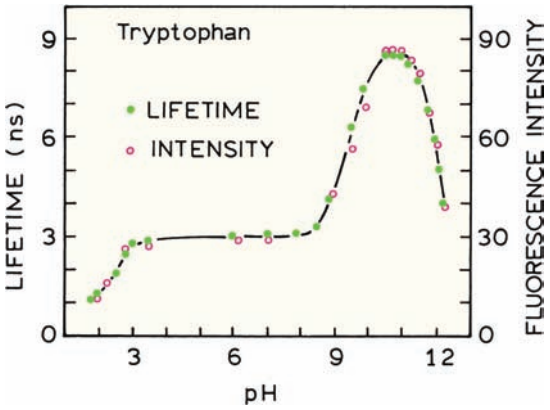

Figure 17.2. Relative fluorescence intensity and mean lifetime of tryptophan as a function of pH. Excitation was 280 nm, and emission through a Corning 0-52 filter. Mean lifetimes were measured from the phase angle at 10 MHz. Revised and reprinted with permission from [25]. Copyright © 1981, American Chemical Society.

is protonated (—NH_3^+) and the carboxy group is ionized (—CO_2^-). In solution the emission of tryptophan can be self-quenched by an intramolecular process involving the indole ring and the positively charged ammonium group. Recall that indole is uniquely sensitive to quenching, particularly by electron-deficient species. Reported quenchers of indole include acrylamide, amides, imidazolium, ammonium, methionine, tyrosine, disulfides, peptide bonds, trifluoroethanol, and electron scavengers.[13–23] Tryptophan can also be quenched by the amino-acid side chains, including glutamine, asparagine, protonated carboxyl groups on glutamate and aspartate, cysteine, and histidine.[24]

Quenching by the ammonium group is seen from the dependence of the tryptophan quantum yield on pH (Figure 17.2). As the pH is increased from 8 to 10 the amino group undergoes dissociation to the neutral form, and the quantum yield and mean lifetime increase approximately threefold.[7,25] This increase in quantum yield and lifetime occurs because the neutral amino group does not quench the indole moiety. The quenching effect of a protonated amino group on tryptophan is general and occurs for a number of tryptophan-containing peptides.[26] Tryptophan analogues lacking the amino group, such as 3-methyl indole[12] or constrained tryptophan derivatives that prevent contact of the amino group with the indole ring,[11] do not show the pH-dependent increase in quantum yield between pH 8 and 10. Complexation of the amino group to a crown ether results in a several-fold increase in fluorescence intensity because the amino group can no longer come in contact with the indole ring.[27] Examination of the pH-dependent intensities of tryptophan indicates that the intensity decreases further below pH 3 and above pH 11. The decrease in intensity below pH 3 is due to intramolecular quenching of indole by the neutral carboxyl group, which serves as an electron acceptor. At high pH indole is quenched by hydroxyl groups, which may be due to collisional quenching by OH^C or by excited-state deprotonation of the proton on the indole nitrogen group.

How does quenching by the amino group explain the bi-exponential decay of tryptophan at pH 7? The quenching process is thought to be most efficient in one of the rotamers, and this species displays the shorter 0.5-ns decay time (Figure 17.1, left). The complete explanation is probably somewhat more complex. For instance, more than three conformations are possible if one considers the possible orientations of the indole ring.[11] Also, it is known that quenching is usually accompanied by transient effects that appear as short components in the intensity decay. Because of the complexity introduced by the amino and carboxyl groups, experiments are frequently performed on uncharged tryptophan analogues (Figure 17.3). In the neutral tryptophan analogue NATA the amino group is acetylated and the carboxyl group converted to an amide. Unchanged tyrosine derivatives are also used (NATyrA). These forms of the amino acids mimic the structures found when these amino acids are contained in a polypeptide chain.

The presence of rotamers is probably the dominant reason for the multi-exponential decay of tryptophan at neutral pH. However, there may be other factors that also contribute to the complex decays of tryptophan and proteins. One of these factors is quenching by peptide bonds.[28] The

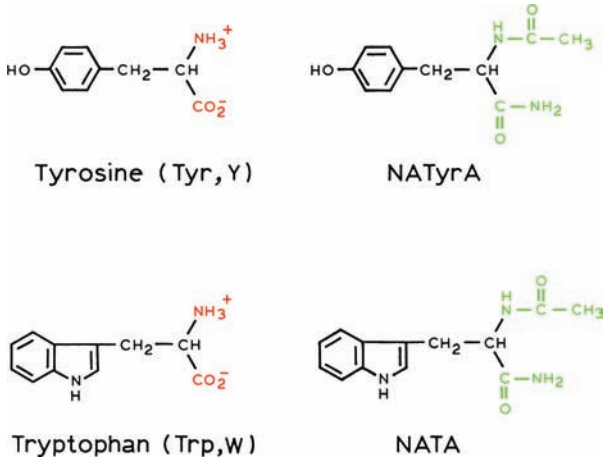

Figure 17.3. Structures of tyrosine and tryptophan and their neutral analogues, N-acetyl-L-tryptophanamide (NATA) and N-acetyl-L-tyrosinamide (NATyrA).

quantum yield of NATA in water is 0.14 and the quantum yield of 3-methyl indole (3-MI) in water is 0.34. The lower quantum yield of NATA is thought to be due to quenching by one or both of the amide groups on NATA (Figure 17.3). If this is true then it is surprising that the rotamer populations of NATA do not result in a multi-exponential decay as occurs in tryptophan. The extent of quenching by amides depends strongly on distance, polarity, and charge distribution surrounding the indole ring and the amide groups. The charge distribution around the tryptophan can either increase or decrease charge separation and quenching by amides. Hence, a variety of effects contribute to the complex intensity decays of proteins.

17.2. TIME-RESOLVED INTENSITY DECAYS OF TRYPTOPHAN AND TYROSINE

Controversy over the intensity decay of tryptophan persisted for many years, and one may wonder why the problem took so long to solve. At that time the measurements pushed the limits of the available instrumentation and methods of data analysis. Many of the early time-resolved decays of tryptophan were measured using flashlamps with nanosecond pulse widths. The low intensities and repetition rates of the flashlamps resulted in data just adequate to detect the short component, but not to reliably resolve its decay time and amplitude. Long data acquisition times were used to obtain the number of photon counts needed to recover the decay components. During this time the flashlamp profiles could change and introduce artifacts. Additionally, it is now known that the 0.5- and 3.1-ns decay components display different emission spectra. Some of the earlier measurements observed only the long-wavelength emission above 360 nm, where the emission from the 0.5-ns component is weak.

The difficulty in resolving the two intensity decay components is illustrated by the intensity decay of tryptophan at pH 7 (Figure 17.4). The light source was a cavity-dumped rhodamine 6G dye laser that was frequency doubled to 295 nm, which provided pulses about 7 ps wide. The detector was a microchannel plate (MCP) PMT detector. The data were fit to the single- and double-exponential models:

$$I(t) = \sum_i \alpha_i \exp(-t/\tau_i) \qquad (17.1)$$

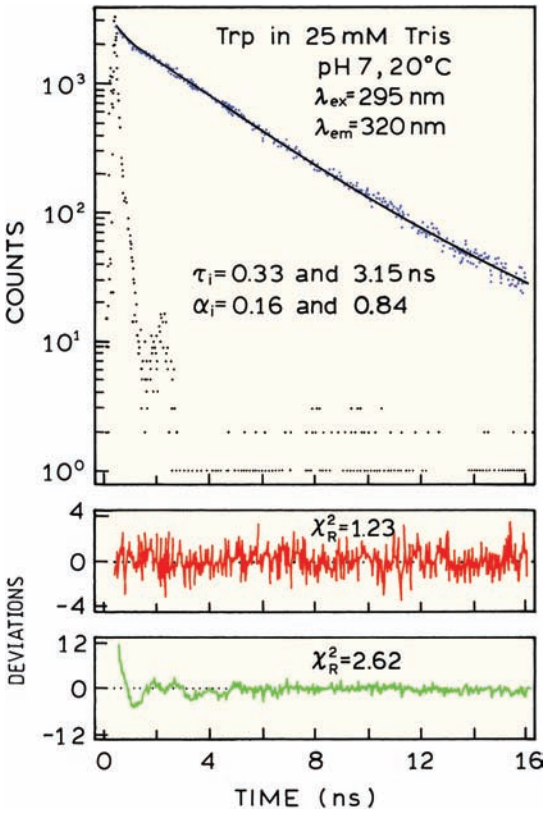

Figure 17.4. Time-domain intensity decay of tryptophan at pH 7. Excitation was at 295 nm, and the emission through a Corning WG 320 filter. The deviations are for the single- ($\chi_R^2 = 2.62$) and double-exponential fit ($\chi_R^2 = 1.23$). From [29].

where α_i are the amplitudes of the components with decay times τ_i. The fitted curves for both the single- and double-exponential models are visually superimposable on the measured data. Deviations of the data from the single-exponential fit are barely visible in the deviations (Figure 17.4, lower panels), and the decrease in χ_R^2 is only from 2.62 to 1.23 for the single- and double-exponential fits, respectively. Even with modern TCSCP instrumentation it remains difficult to resolve the two decay times of tryptophan.

The multi-exponential decay of tryptophan can also been observed using the frequency-domain method (Figure 17.5). The data were obtained using the same dye laser light source, a MCP PMT detector, and the harmonic content method (Chapter 5). The deviations from the single-exponential model are clearly non-random (lower panels). The 50-fold decrease in χ_R^2 for the double-exponential fit from 58.9 to 0.9 is convincing evidence for the non-single-exponential decay of tryptophan.

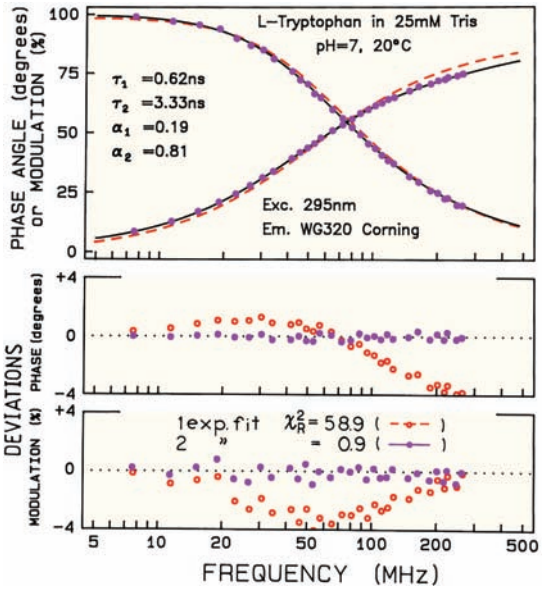

Figure 17.5. Frequency-domain intensity decay of tryptophan in H_2O at 20°C and pH 7. Excitation at 295 nm. The emission was collected through a long pass Corning WG 320 filter. From [2].

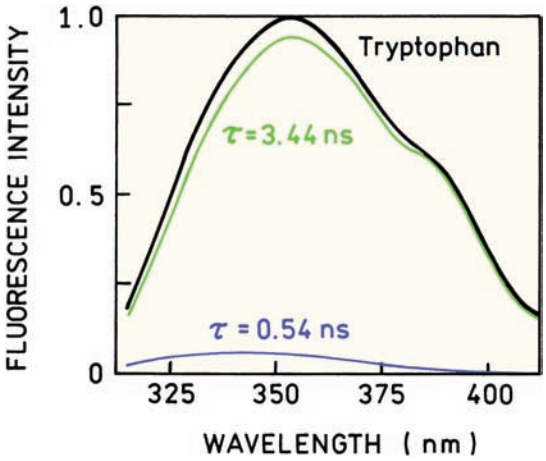

Figure 17.6. Spectral resolution of the short and long ns decay components of tryptophan. Similar results were reported in [5–6]. From [30].

17.2.1. Decay-Associated Emission Spectra of Tryptophan

Suppose a sample displays a multi-exponential decay, and that the decay is different at different emission wavelengths. The intensity decay is then described by

$$I(\lambda,t) = I(t) = \sum_i \alpha_i(\lambda)\, \exp(-t/\tau_i) \qquad (17.2)$$

where $\alpha_i(\lambda)$ are the wavelength-dependent pre-exponential factors and τ_i the decay times. This expression assumes the decay times are independent of wavelength. The emission spectrum due to each component can be calculated using

$$I_i(\lambda) = \frac{\alpha_i(\lambda)\tau_i I(\lambda)}{\sum_j \alpha_j(\lambda)\tau_j} \qquad (17.3)$$

In this expression $I(\lambda)$ is the steady-state emission spectrum. The product $\alpha_i(\lambda)\tau_i$ appears in the numerator because the steady-state intensity is proportional to this product. The sum in the denominator is proportional to the total intensity at this wavelength. These spectra $I_i(\lambda)$ are called decay-associated spectra (DAS) because they represent the emission spectrum of the component emitting with lifetime τ_i.

The multi-exponential decays recovered for each emission wavelength are used to construct the emission spectra associated with each decay time. To calculate the decay-associated spectra one has to recall that the fractional contribution (f_i) of each species to the steady-state intensity is proportional to the product $\alpha_i\tau_i$. The contribution of a short-decay-time component to the steady-state intensity is lower than the relative amplitude (α_i) of the short-decay-time component in the intensity decay. In the case of tryptophan the short component contributes only about 4% to the total emission of tryptophan at neutral pH (Figure 17.6). Emission from the short component is centered near 335 nm and occurs at slightly shorter wavelengths than for the overall emission. This blue shift of the emission is consistent with the expected effect of a nearby positive charge on the polar ^1L_a state of indole. Little contribution from the ^1L_b state is expected, as conversion of ^1L_b to ^1L_a occurs in less than 2 ps.[31]

17.2.2. Intensity Decays of Neutral Tryptophan Derivatives

In proteins the amino and carboxyl groups of tryptophan are converted into neutral groups by the formation of peptide bonds. The quenching effect of the α-amino group is no longer present. Neutral tryptophan analogues typically display simpler decay kinetics than tryptophan itself. The most commonly used analogue is N-acetyl-L-tryptophanamide, which has essentially the same structure as a tryptophan residue in proteins (Figure 17.3). The intensity decay of

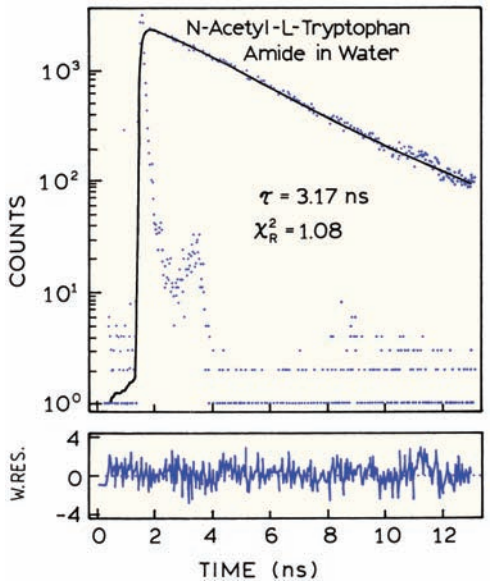

Figure 17.7. Time-domain intensity decay of N-acetyl-L-tryptophanamide (NATA) at pH 7. From [29].

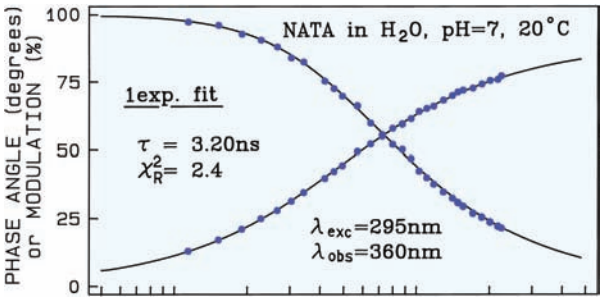

Figure 17.8. Frequency-domain intensity decay of NATA at pH 7, 20°C. The solid curves are for the single-exponential fit, τ = 3.20 ns, χ_R^2 = 2.4. The double-exponential fit yielded τ_1 = 1.04 ns, τ_2 = 3.28 ns, α_1 = 0.05 and α_2 = 0.95, with χ_R^2 = 1.3. From [29].

NATA (Figure 17.7) is essentially a single exponential.[6,12,32] Comparable frequency-domain data for NATA also revealed a dominant single-exponential decay (Figure 17.8). There is some decrease in χ_R^2 for the double-exponential fit, so that the decay of NATA may display a weak second component. However, for all practical purposes NATA displays a single decay time (Table 17.1).

17.2.3. Intensity Decays of Tyrosine and Its Neutral Derivatives

Tyrosine can also display complex decay kinetics, but its properties are opposite to that of tryptophan. Frequency-domain intensity decays of tyrosine and its neutral analogue N-acetyl-L-tyrosinamide (NATyrA) are shown in Figure 17.9. Tyrosine itself displays a single-exponential decay,[33–34] whereas NATyrA displays a bi-exponential decay (Table 17.1). The molecular origin of the double-exponential decay of NATyrA is not clear but may be due to the presence of ground state rotamers.[35–37] The peptide bonds or carbonyl groups may quench the phenol emission by an electron-transfer mechanism.[38–39] Considerably less information is available on the intensity decays of phenylalanine.[40–42] pH-dependent lifetimes have not been reported.

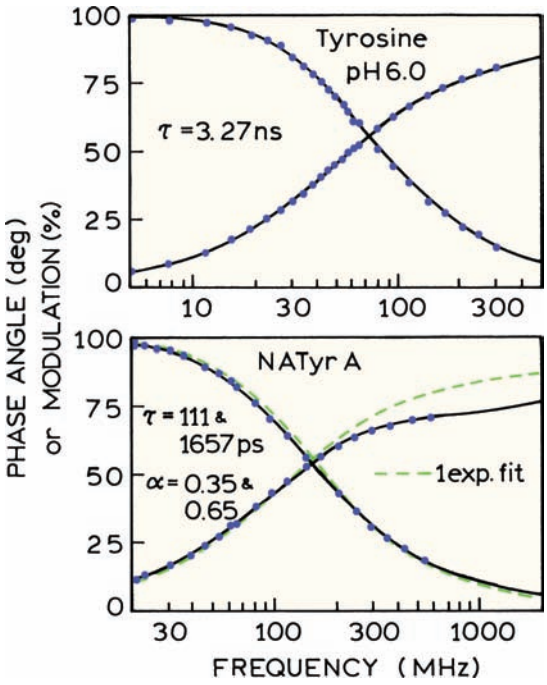

Figure 17.9. Frequency-domain intensity decays of tyrosine and NATyrA. Data reprinted with permission from [33]. Copyright © 1987, American Chemical Society.

The intensity decay of tyrosine in water is usually a single exponential, but different results can be obtained at different observation wavelengths (Figure 17.10). These intensity decays were measured using 277-nm excitation from a frequency-tripled Ti:sapphire laser and a microchannel plate PMT detector. For the peak tyrosine emission at 310 nm the intensity decay is a single exponential.[43] As the observation wavelength increases the plots become curved, showing the presence of additional components. The component with a decay time of 0.98 ns is due to tyrosinate, which forms during the excited-state lifetime. This component from tyrosine is seen as the rapidly decaying species at

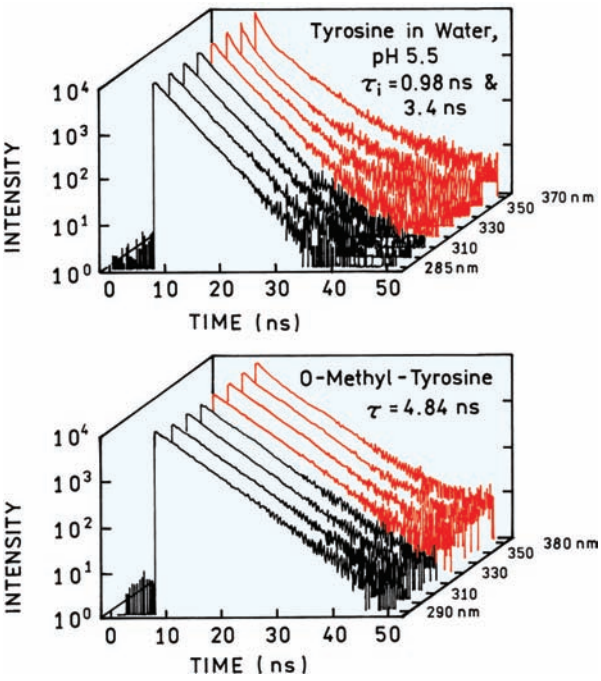

Figure 17.10. Wavelength-dependent intensity decays of tyrosine and o-methyl-tyrosine in water at pH 5.5. For tyrosine the upward curvature at long times and long wavelengths is thought to be due to impurities. Revised and reprinted with permission from [43]. Copyright © 2004, American Chemical Society.

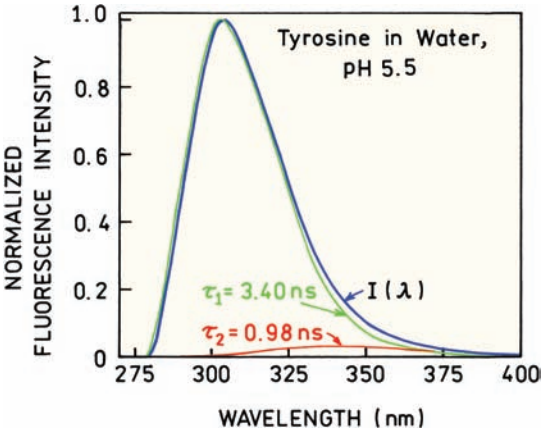

Figure 17.11. Decay-associated spectra of tyrosine in water at pH 5.5. From [43].

short times and long wavelengths. Ionization of the hydroxyl group occurs because its pK_a decreases to about 4 in the excited state. The assignment of this component to ionized tyrosine is supported by the intensity decays of O-methyl-tyrosine (Figure 17.10, lower panel), which do not show this component. The DAS for the two main components in the tyrosine decay are shown in Figure 17.11. The dominant emission centered at 310 nm is associated with the 3.40-ns component. The 0.98-ns component is due to a longer-wavelength emission centered near 360 nm, which is emission from tyrosinate.

17.3. INTENSITY AND ANISOTROPY DECAYS OF PROTEINS

We now consider the intensity decays of tryptophan residues in proteins. Since NATA displays a single decay time, we can expect single-tryptophan proteins to display single-exponential decays. However, this is not the case. In a survey of eight single-tryptophan proteins, only one protein (apo-azurin) was found to display a single decay time.[3] This early report was confirmed by many subsequent studies showing that most single-tryptophan proteins display double or triple-exponential decays (Table 17.2), and of course multi-tryptophan proteins invariably display multi-exponential decays (Table 17.3).

What are the general features of protein intensity decays? The variability of the intensity decays is a result of protein structure. The intensity decays and mean decay times are more variable for native proteins than for denatured proteins. The decay times for denatured proteins can be grouped into two classes, with decay times near 1.5 and 4.0 ns, with the latter displaying a longer emission wavelength.[3] This tendency is enhanced in native proteins, and many of them show lifetimes as long as 7 ns, typically on the red side of the emission. Surprisingly, buried tryptophan residues seem to display shorter lifetimes. The longer lifetimes of exposed tryptophan residues have been puzzling because exposure to water is expected to result in shorter lifetimes. It is now known that peptide bonds can quench tryptophan emission.[28] Hence, the shorter lifetimes of

Table 17.2. Intensity Decays of Single-Tryptophan Proteins[a]

Protein	τ_1 (ns)	τ_2 (ns)	τ_3 (ns)	Ref.
Azurin	4.8	0.18	–	4
Apoazurin	4.9	–	–	4
Staph. nuclease	5.7	2.0	–	3
RNase T_1 (pH 5.5)	3.87	–	–	–
RNase T_1 (pH 7.5)	3.57	0.98	–	–
Glucagon	3.6	1.1	–	4
Human serum albumin	7.8	3.3	–	4
Phospholipase A2	7.2	2.9	0.96	4
Subtilisin	3.82	0.83	0.17	44

[a]Additional intensity decays of single-tryptophan proteins can be found in [45].

Table 17.3. Intensity Decays of Multi-Tryptophan Proteins[a]

Protein	# of Trps	τ_1 (ns)	τ_2 (ns)	τ_3 (ns)
Bovine serum albumin	2	7.1	2.7	–
Liver alcohol dehydrogenase	2	7.0	3.8	–
Ferredoxin	2	6.9	0.5	–
Sperm whale myoglobin	2	2.7	0.1	0.01
Papain	5	7.1	3.7	1.1
Lactate dehydrogenase	6	8.0	4.0	1.0

[a]From [4].

buried residues may be because the buried tryptophan residues have more contact with peptide bonds than the exposed residues. However, there is little correlation between the mean lifetime and emission maximum of proteins (see Figure 16.12). In proteins that contain chromophoric groups (ferredoxin and myoglobin), the tryptophan residues are often quenched by resonance energy transfer, resulting in subnanosecond decay times (Table 17.3).

Multi-exponential decays are not surprising for multi-tryptophan proteins. However, the origin of multi-exponential decays in single-tryptophan proteins is less clear. Given that NATA displays a single decay time, it seems that a single-tryptophan residue in a single unique protein environment should result in a single decay time. One possible origin of multi-exponential decays is the existence of multiple protein conformations. Since nearby amino-acid residues can act as quenchers, it seems logical that slightly different conformations can result in different decay times for native proteins. However, multi-exponential decays can be observed even when the proteins are thought to exist in a single conformation.[46-47] As shown in the following section, unfolding of a protein can change a single-exponential decay into a multi-exponential decay, which seems to be consistent with the presence of multiple conformations for a random coil peptide. It appears that multi-exponential decays of single-tryptophan proteins can result in part from dynamic processes occurring during the excited-state lifetime.[48–49] These dynamic processes can include nearby motion of quenchers, spectral relaxation, and/or resonance energy transfer.

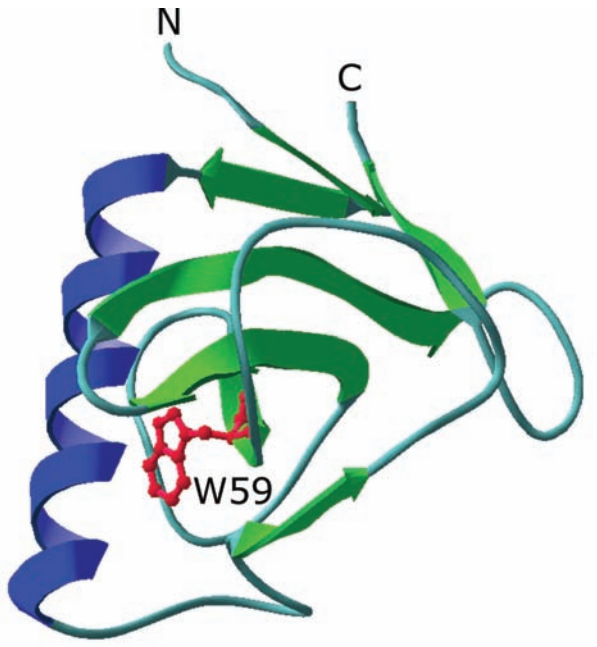

Figure 17.12. Structure of ribonuclease T_1 in the presence of 2'-GMP (2'-GMP removed). Trp 59 is located between the α-helix and β-sheet structure.

17.3.1. Single-Exponential Intensity and Anisotropy Decay of Ribonuclease T_1

In the previous section we saw that most single-tryptophan proteins display multi-exponential decays. However, there are two known exceptions—apoazurin and ribonuclease T_1 from *Aspergillus oryzae*. Most ribonucleases do not contain tryptophan. Ribonuclease T_1 is unusual in that it contains a single-tryptophan residue, and under some conditions displays a single-exponential decay. RNase T_1 consists of a single polypeptide chain of 104 amino acids (Figure 17.12). RNase T_1 has four phenylalanines, nine tyrosines, and a single-tryptophan residue at position 59. This tryptophan residue is near the active site. The emission maximum is near 323 nm, suggesting that this residue is buried in the protein matrix and not exposed to the aqueous phase. Quenching studies have confirmed that this residue is not easily accessible to quenchers in the aqueous phase.[50–53] Ribonuclease is also unusual in that its intensity decay is a single exponential at pH 5.5[54–57] (Figure 17.13, top). The decay becomes a double exponential at pH 7. A single-exponential decay is convenient because changes in the protein structure can be expected to result in more complex decay kinetics. It is easier to detect a single-exponential decay becoming a multi-exponential decay than it is to detect a change in a multi-exponential decay.

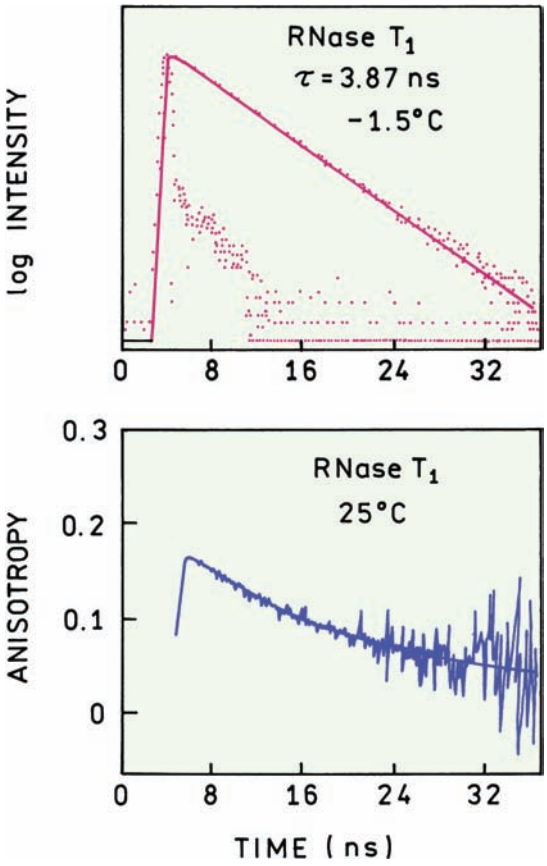

Figure 17.13. Time-resolved fluorescence intensity and anisotropy decay of RNase T_1 in buffered aqueous solution pH 5.5. Excitation at 295 nm. Data from [54].

17.3.2. Annexin V: A Calcium-Sensitive Single-Tryptophan Protein

Ribonuclease T_1 provided an example of a single-tryptophan protein that displayed single-exponential intensity and anisotropy decays (Figure 17.13, bottom). For most proteins, even with a single-tryptophan residue, the intensity and anisotropy decay are more complex. One example is annexin V, which possesses a single-tryptophan residue (Figure 17.14). Annexins are a class of homologous proteins that bind to cell membranes in a calcium-dependent manner. The crystal structure is known to be different with and without bound calcium.[58] The emission from the single-tryptophan residue is sensitive to calcium.[59] Addition of calcium results in shift of the emission maximum from 324 to 348 nm (Figure 17.15).

In the absence of calcium the intensity decay is highly non-exponential (Figure 17.16). Addition of calcium causes the intensity decay to become more like a single exponential. This dramatic change in calcium suggests the presence of a nearby quenching group in the calcium-free form. The crystal structures of annexin V are consistent with this suggestion because the tryptophan residue moves away from the protein in the presence of calcium (Figure 17.14).

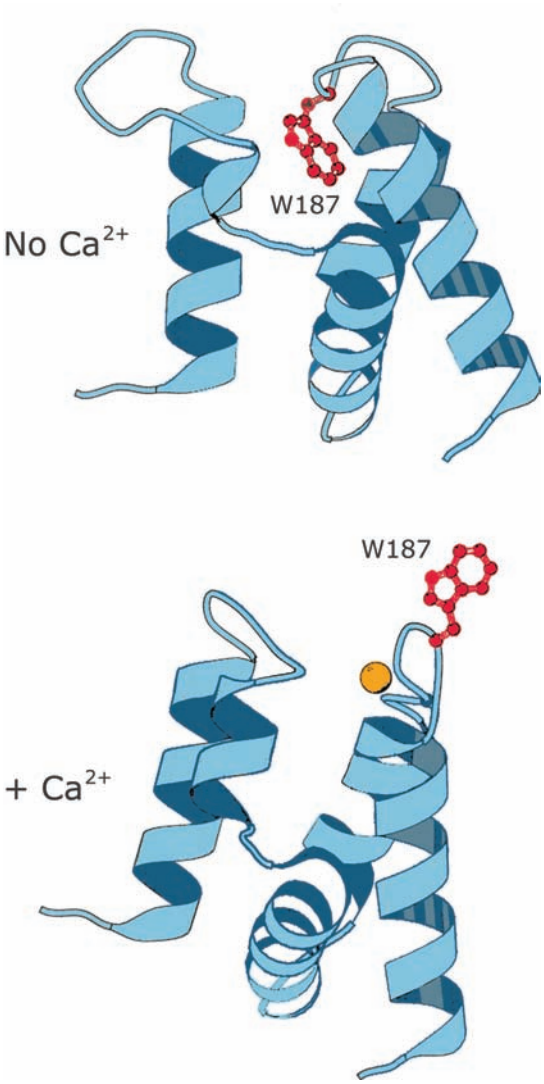

Figure 17.14. Structure of Annexin V in the absence (top) and presence (bottom) of Ca^{2+}. The calcium atom is shown in red. Revised and reprinted with permission from [60]. Copyright © 1994, American Chemical Society.

As was described in Chapter 4 the multi-exponential model can be used to fit almost any intensity decay, even if the actual decay has some other functional form. When examining tables of multi-exponential decay parameters it is difficult to obtain an intuitive vision of the decays from the numerical values. The forms of complex intensity decays can be visualized from the lifetime distributions.

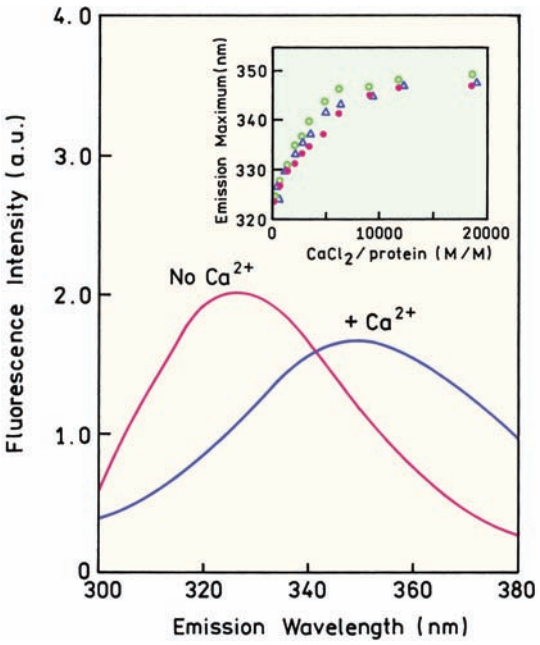

Figure 17.15. Fluorescence emission spectrum of trp 187 in annexin V with and without calcium-bound protein. The insert shows the dependence of the emission maximum of annexin V on the calcium-to-protein molar ratio under several conditions. Revised and reprinted with permission from [59]. Copyright © 1994, American Chemical Society.

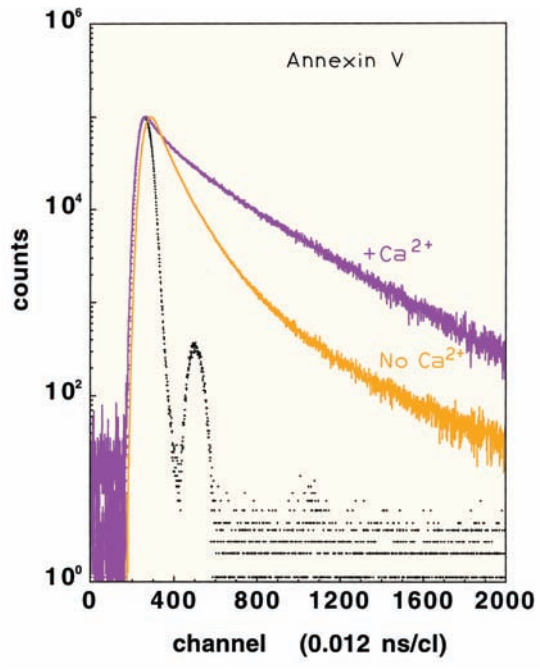

Figure 17.16. Fluorescence intensity decays of trp 187 in annexin V in the absence and presence of calcium. The intensity decays were measured at 320 nm without calcium and 350 nm with calcium. Revised and reprinted with permission from [59]. Copyright © 1994, American Chemical Society.

Figure 17.17 show the lifetime distributions of annexin V in the absence and presence of calcium. These plots shows the amplitude of the intensity decay for each decay time. The lifetime axis is logarithmic, as is common with maximum entropy analyses. The more rapid intensity decay in the absence of calcium can be understood from the decay component near 0.2 ns seen in the lifetime distribution. Binding of calcium to annexin V results in the appearance of a larger decay time component near 4 ns.

The calcium-dependent change in tryptophan exposure is expected to affect the anisotropy decay. As expected for a surface-exposed residue, the anisotropy decay also becomes more rapid in the presence of calcium (Figure 17.18). Once again it is helpful to visualize these decays as distributions, in this case distributions of correlation times. In the absence of calcium the anisotropy decay of annexin V is mostly due to overall rotational diffusion with a correlation time near 12 ns. In the presence of Ca^{2+} the anisotropy decay shows three correlation times near 80 ps, 1.2 ns, and 12 ns (Figure 17.19). Taken together these results are consistent with the

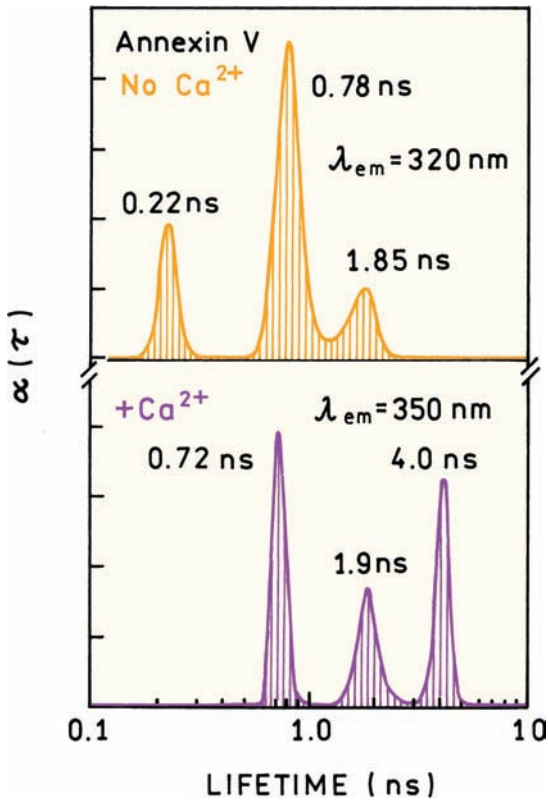

Figure 17.17. Lifetime distributions for the tryptophan emission from Annexin V in the absence and presence of calcium. The distributions were recovered using the maximum entropy method. Data from [60].

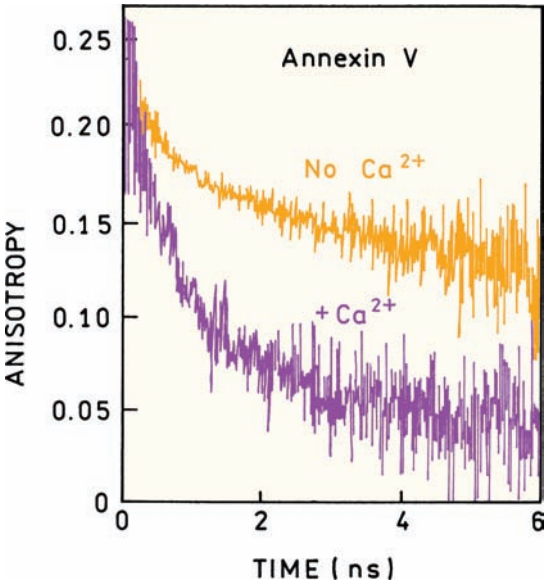

Figure 17.18. Time-resolved anisotropy decay of Annexin V in the absence and presence of calcium. Data from [59]; figure provided by Dr. Jacques Gallay from the Paris-Sud University, France.

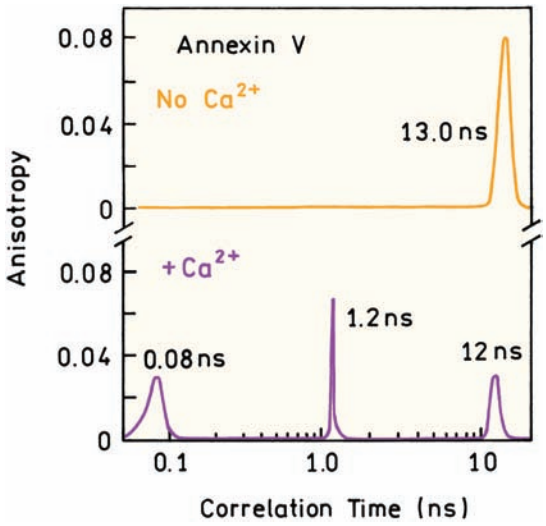

Figure 17.19. MEM-reconstituted correlation time distribution of trp 187 in annexin V. Data from [59].

known structural change induced by Ca^{2+}, which results in displacement of the trp 187 from a buried environment to an exposed environment in which the side chain is extended into the aqueous phase (Figure 17.14). It is apparent that the time-resolved intensity and anisotropy decays are highly sensitive to protein conformation.

17.3.3. Anisotropy Decay of a Protein with Two Tryptophans

From the previous examples we saw that in different proteins the tryptophan residues can be rigidly held by the protein or display segmental motions independent of overall rotational diffusion. In a multi-tryptophan protein residues, each residue may be rigid or mobile. This type of behavior is seen for single-tryptophan mutants of the IIA^{Glc} protein.[61] This protein from *E. coli* is involved in transfer of phosphate groups, so we will call it the phosphoryl-transfer protein (PTP).

X-ray diffraction of the PTP shows a well-defined structure from residues 19 to 168. Residues 1 to 18 are not seen in the x-ray structure and are thus mobile in the crystal, and probably also in solution. Wild-type PTP does not contain any tryptophan residues. Single-tryptophan mutants were prepared with residues at positions 3 and 21, which were expected to be in the mobile and rigid regions, respectively. Time-resolved anisotropy decay of these mutant proteins are shown in Figure 17.20. At times longer than 3 ns both mutants display long correlation (θ_L) times near 40 ns. This correlation time is larger than expected for a protein with a molecular weight near 21 kDa (Table 10.4), which may be due to the flexible chain. The mutants show very different behavior at times below 3 ns, where the F3W mutants display short correlation times (θ_S) near 1 ns. The short correlation time is due to motion of residues 1–18,

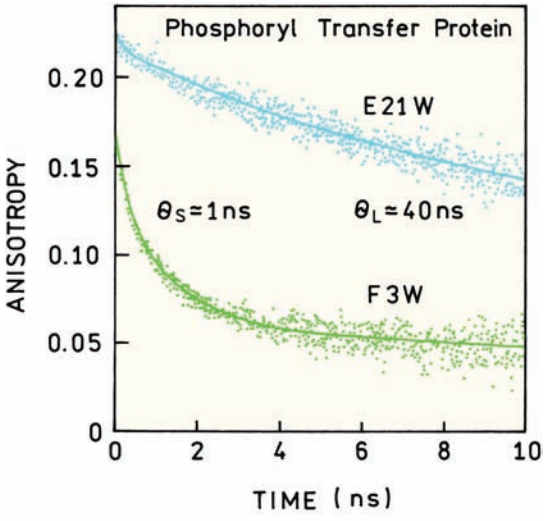

Figure 17.20. Time-resolved anisotropy decays of single-tryptophan mutants of the phosphoryl transfer protein. 296-nm excitation was obtained from a cavity-dumped frequency-doubled dye laser. Revised from [61].

Table 17.4. Anisotropy Decays of NATA and Single-Tryptophan Peptides and Proteins[a]

Proteins	θ_1 (ps)	θ_2 (ps)	r_{01}	r_{02}
RNase T_1, 20°C	6520	–	0.310	–
Staph. nuclease	10160	91	0.303	0.018
Monellin	6000	360	0.242	0.073
ACTH	1800	200	0.119	0.189
Gly-trp-gly	135	39	0.105	0.220
NATA	56	–	0.323	–
Melittin monomer	1730	160	0.136	0.187
Melittin tetramer	3400	60	0.208	0.118

[a]20°C, excitation at 300 nm. From [77] and [78].

which are independent of the compact domain of the protein. These results show how tryptophan residues at different locations within the same protein can have different motions and different anisotropy decays.

17.4. PROTEIN UNFOLDING EXPOSES THE TRYPTOPHAN RESIDUE TO WATER

The spectral properties of proteins are dependent upon their three-dimensional structure. This dependence can be seen by measuring the emission of native and denatured proteins. The effects of denaturation are easy to observe for ribonuclease T_1 (Figure 17.12), which displays single-exponential intensity and anisotropy decays in the native conformation (Figure 17.13). Emission spectra of ribonuclease T_1 (RNase T_1) are shown in Figure 17.21. An excitation wavelength of 295 nm was chosen to avoid excitation of the tyrosine residues. For the native protein the emission maximum is at 323 nm, which indicates the indole group in a nonpolar environment. Although not evident in Figure 17.21, others have reported the presence of weak vibrational structure in the emission spectrum,[54] as was seen for indole in cyclohexane and for azurin.

Proteins can be unfolded at high temperature or by the addition of denaturants such as urea or guanidine hydrochloride. These conditions result in a dramatic shift in the emission spectra of RNase T_1 to longer wavelengths. In the presence of 7.0 M guanidine hydrochloride, or at 65°C, the emission spectrum of RNase T_1 shifts to longer wavelength to become characteristic of a tryptophan residue that is fully exposed to water (Figure 17.21). These results show that protein structure determines the emission maximum of proteins or, conversely, that protein folding can be studied by changes in the intensity or emission spectra of proteins.

17.4.1. Conformational Heterogeneity Can Result in Complex Intensity and Anisotropy Decays

Frequency-domain measurements were used to study the intensity decays of native and denatured Rnase T_1 (Figure 17.22). In the native state at pH 5.5 the frequency-domain data reveal a single-exponential decay with τ = 3.92 ns. When the protein is denatured by heat the intensity decay becomes strongly heterogeneous.

Protein unfolding also affects the anisotropy decays of RNase T_1. The frequency-domain data for Rnase T_1 at 5°C is characteristic of a single correlation time (Figure 17.23). If the temperature is increased, or if one adds denaturant, there is an increase in the high-frequency differential phase angles and a decrease in the modulated anisotropy. These effects in the frequency-domain anisotropy data are charac-

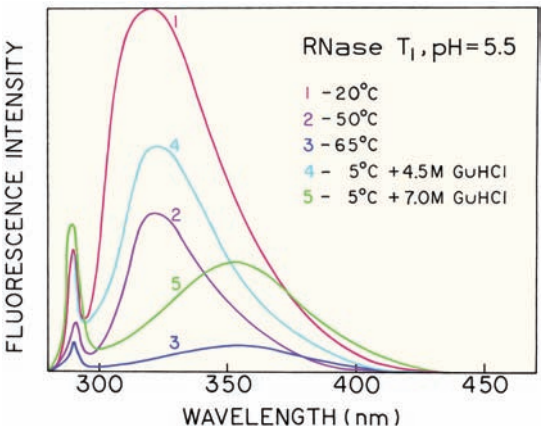

Figure 17.21. Emission spectra of ribonuclease T_1 (RNase T_1), λ_{ex} = 295 nm. From [62].

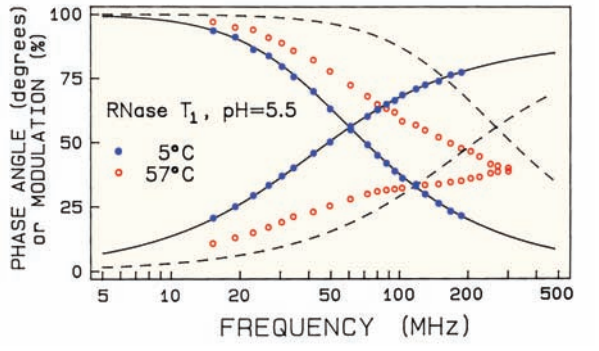

Figure 17.22. Frequency response of RNase T_1 at 5 (●) and 57°C (○). The solid and dashed lines show the best single component fits to the data at 5 and 57°C, respectively. The χ_R^2 values were 1.3 at 5°C and 2082 at 57°C. From [55].

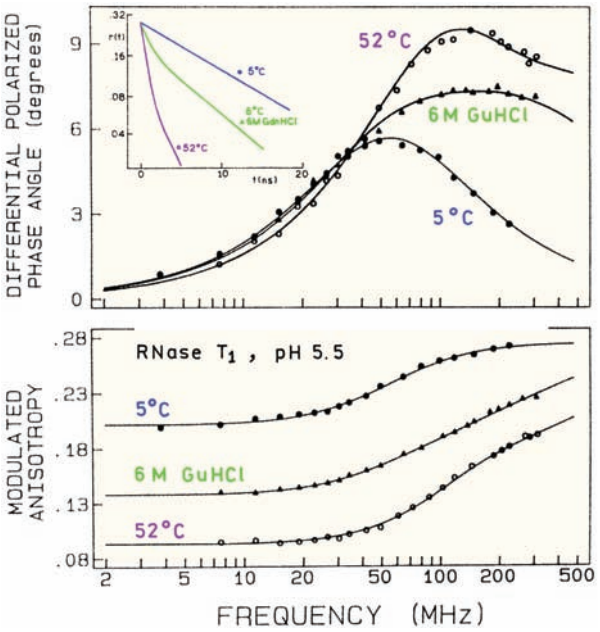

Figure 17.23. Frequency-domain anisotropy decays of RNase T_1 (pH 5.5) at 5°C (●) and 52°C (○) and at 5°C with 6 M guanidine hydrochloride (▲). The insert shows equivalent time-dependent anisotropies reconstructed from the FD data. Similar data were reported in [63]. From [2].

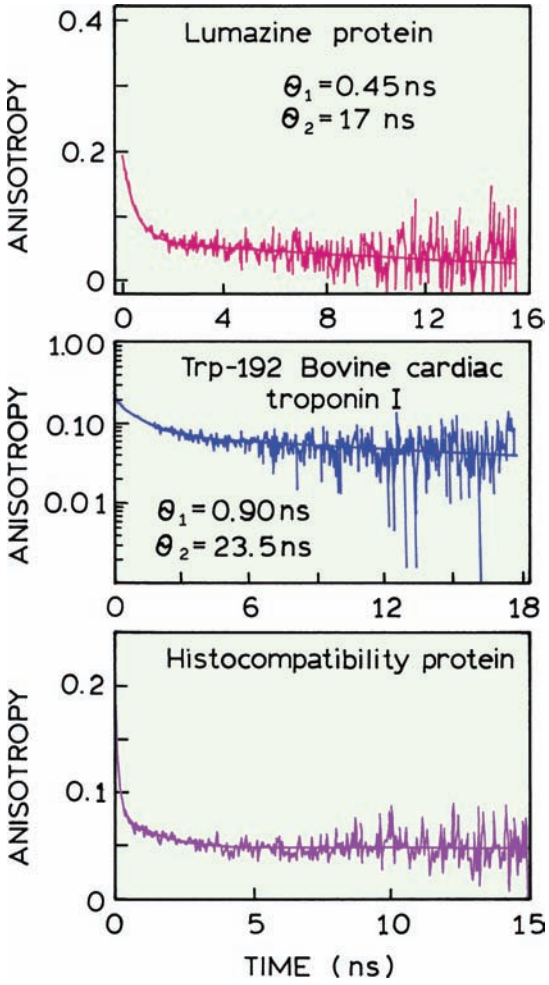

Figure 17.24. Anisotropy decay for the single-tryptophan residue in the lumazine protein (top), for trp-192 in bovine cardiac troponin I (middle) and for a histocompatibility protein (bottom). Revised from [74], [75], and [76].

teristic of rapid motions of the residue in addition to slower overall rotational diffusion. At low frequency the modulated anisotropies are equal to the steady-state anisotropies. At high frequencies the modulated anisotropies approach the fundamental anisotropy (r_0). The FD anisotropy data can be used to reconstruct the time-dependent anisotropy decays (insert). In the native state the anisotropy decay is a single exponential. When unfolded by either guanidine hydrochloride or high temperature, the anisotropy decay displays a fast component due to segmental motions of the tryptophan residue. Hence, rapid components in the anisotropy decay can be expected for random coil peptides, or for tryptophan residues on the surfaces of proteins that are not constrained by the three-dimensional structure.

17.5. ANISOTROPY DECAYS OF PROTEINS

Proteins display a variety of anisotropy decays. Most proteins show fast components in the decays at early times.[63–78] Typical anisotropy decays are shown in Figure 17.24. The single tryptophan in the lumazine protein shows a high degree of segmental flexibility. The long component near 17 ns is assigned to overall rotational diffusion of the protein. The short component near 0.45 ns is assigned to rapid motions of the tryptophan residue independent of overall rotational diffusion. Another example is the tryptophan residue in bovine troponin I, which shows a shorter correlation time near 0.90 ns and a correlation time of 23.5 ns due to overall rotational diffusion. In many cases the rapid components in the anisotropy decay are too fast to be measured, as shown for a histocompatibility complex protein. In this case about 75% of the anisotropy is lost due to rapid motions. The short correlation time observed in proteins is variable and ranges from 50 to 500 ps, with the values being determined in part by the time resolution of the instrument. The shorter correlation time is approximately equal to that observed for NATA in water or for small peptides (Table 17.4). These shorter correlation times are typically insensi-

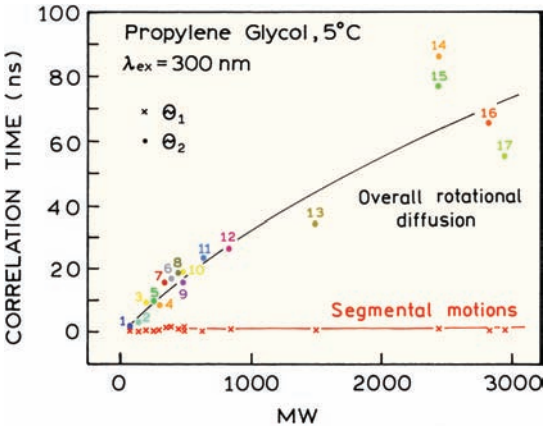

Figure 17.25. Short and long rotational correlation times for indole, tryptophan, and peptides in propylene glycol at 5°C. 1, indole; 2, 3-methylindole; 3, trp; 4, NATA; 5, gly-trp; 6, trp-trp; 7, gly-trp-gly; 8, leu-trp-leu; 9, glu-trp-glu; 10, lys-trp-lys; 11, gastrin; 12, pentagastrin; 13, [tyr^4-bombesin); 14, dynorphin; 15, [asn^{15}]-dynorphin; 16, cosyntropin; 17, melittin. From [79].

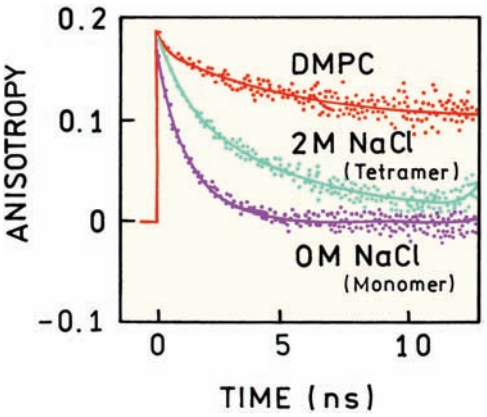

Figure 17.26. Anisotropy decays of monomeric and tetrameric melittin, in water and 2 M NaCl, respectively. Also shown is the anisotropy decay when bound to DMPC lipid vesicles. Excitation at 300 nm. Data from [80].

tive to protein folding and are not greatly affected by the viscosity of the solution.

The picosecond component in the anisotropy decays of proteins display some characteristic features. Their fraction of the total anisotropy is typically larger for small unstructured peptides than for tryptophan residues buried in a protein matrix. Unfolding of a protein usually increases the amplitude of the fast motions. The magnitude of the short correlation time seems to be mostly independent of the size of the protein or peptide. This is shown in Figure 17.25, which shows the two correlation times recovered for molecules ranging from indole, to tryptophan, to the tripeptide lys-trp-lys, to melittin.[79] The molecules were dissolved in propylene glycol, so the overall correlation times are longer than those found with water. The longer correlation time increases with molecular weight. However, the rapid correlation time is independent of molecular weight and is near 0.5 ns for all peptides.

17.5.1. Effects of Association Reactions on Anisotropy Decays: Melittin

The single-tryptophan peptide melittin provides a good example of how a protein anisotropy decay depends on the association with other biomolecules. In the presence of high salt concentration, melittin self-associates from monomers to tetramers. During this process the single-tryptophan residue on each chain is buried in the center of the four-helix bundle. The anisotropy decay changes due to the larger overall size and restriction of segmental motions. Anisotropy decays for melittin have been reported by several laboratories.[80–82] Typical data for the monomer and tetramer are shown in Figure 17.26. The anisotropy decay was multi-exponential in both cases, with a 20–40-ps component in either state. The anisotropy decays more slowly in 2 M NaCl, where melittin forms a homotetramer. The longer global correlation time was 1.4 ns for the monomer and 5.5 ns for the tetramer, which are consistent with overall rotational diffusion.

Melittin binds to lipid vesicles because one side of the protein has nonpolar surface in the α-helical state.[83–85] This binding results in a dramatic change in the anisotropy decay (Figure 17.26), which now shows a correlation time near 12 ns, but with uncertainty in the actual value.[80] It is difficult to obtain much information after 10 ns, or three times the mean lifetime, due to the low remaining intensity. In general one should select probes whose decay times are longer than the process being measured.

The data in Figure 17.26 illustrate a difficulty frequently encountered when measuring protein anisotropy decays. The measured time-zero anisotropy, $r(0)$, is less than the fundamental anisotropy ($r_0 = 0.3$) for the 300-nm excitation wavelength. A low apparent time-zero anisotropy can be due to the limited time resolution of the instrumentation. If the correlation time is too short, the anisotropy decays within the instrument response function and the apparent time-zero anisotropy is less than the actual value.[86]

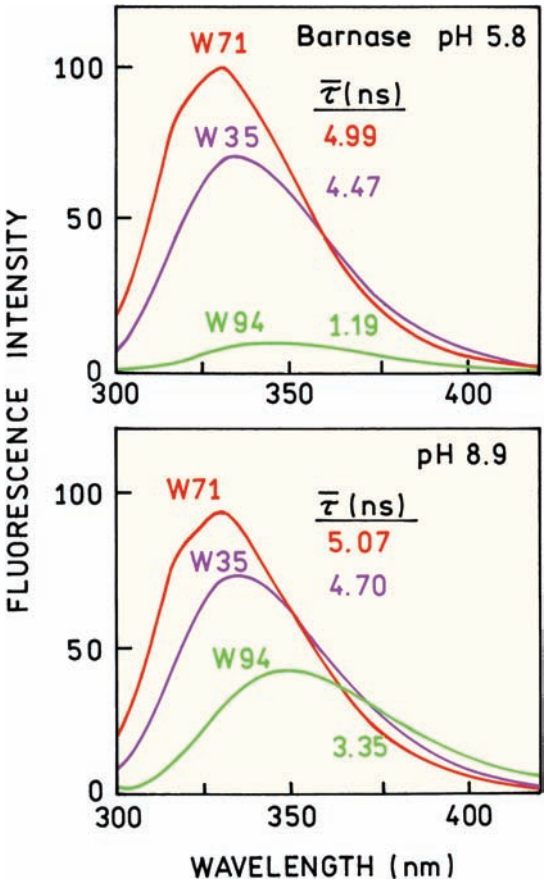

Figure 17.27. Emission spectra and mean decay time of the three single-tryptophan mutants of barnase at pH 5.8 and 8.9. The mean lifetimes are different than in [87] and were calculated using $\bar{\tau} = 3f_i\tau_i$. Data from [87].

17.6. BIOCHEMICAL EXAMPLES USING TIME-RESOLVED PROTEIN FLUORESCENCE

17.6.1. Decay-Associated Spectra of Barnase

In Section 16.8.2 we described the spectral properties of barnase. The wild-type protein contains three tryptophan residues: W35, W71, and W94 (Figure 16.48). Barnase displays a pH-dependent change in intensity that was attributed to quenching of W94 by the side chain of a protonated histidine residue H18. Time-resolved measurements and site-directed mutagenesis were used to determine the lifetimes of W94 when the histidine is positively charged or in the neutral state. This was accomplished by constructing three double mutants, each containing a single-tryptophan residue.[87] The intensity decays of all the single-tryptophan mutants were multi-exponential. The emission spectra and

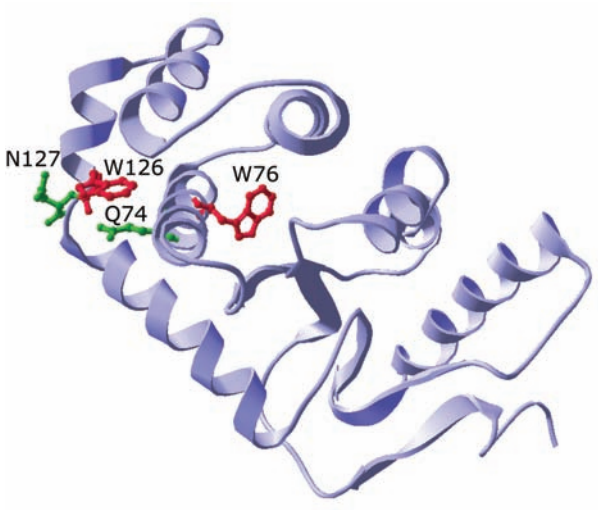

Figure 17.28. Structure of disulfide oxidoreductase DsbA from *E. coli*.

mean lifetimes are shown in Figure 17.27. The mean lifetimes of W71 and W35 are essentially independent of pH. The mean lifetime of W94 changes dramatically with pH, from 1.19 ns at pH 5.8 to 3.35 ns at H 8.9. This effect is due to H18, which quenches W94 when in the protonated form. These results confirm the conclusions obtained using the mutants that contained two tryptophan residues (Section 16.8.2).

17.6.2. Disulfide Oxidoreductase DsbA

The emission of tryptophan residues in proteins is frequently affected by nearby groups in proteins. Such effects were seen in the disulfide oxidoreductase DsbA from *E. coli*.[88–89] The wild-type DsbA contains two tryptophan residues: W76 and W126 (Figure 17.28). W76 is sensitive to the redox state of DsbA. W126 was found to be essentially nonfluorescent irrespective of the redox state of the protein. The reason for quenching of W126 in DsbA was studied using site-directed mutagenesis. The mutant protein W76F was constructed to obtain a protein that contained only W126. The origin of the quenching was studied using W76F by mutating amino-acid residues close to W126. Since amides are known to be possible quenchers of tryptophan, glutamine 74 and asparagine 127 were replaced with alanine.

The time-resolved intensity decays of the DsbA mutants were measured for various wavelengths across the emission spectra. The recovered multi-exponential decays

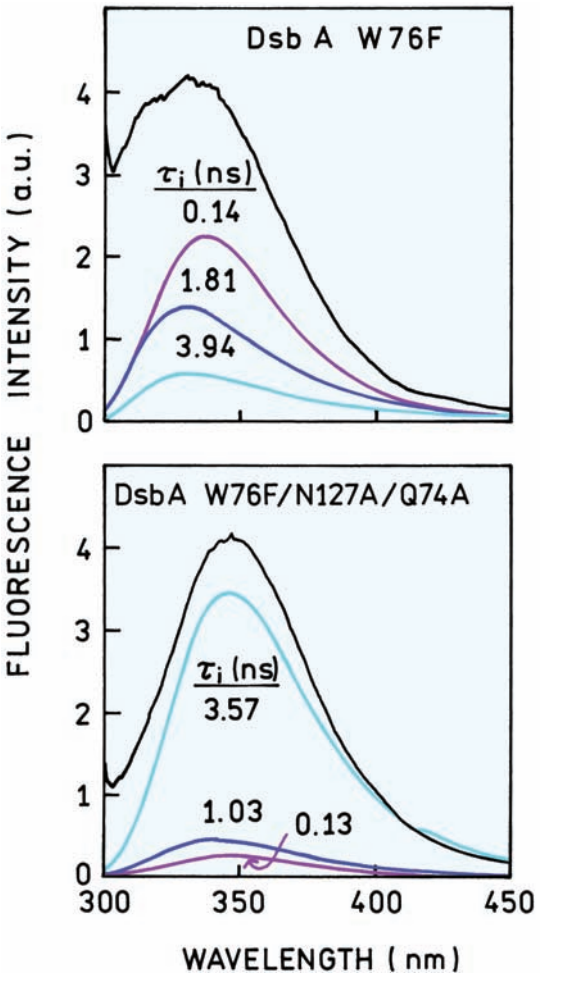

Figure 17.29. Steady-state emission and decay-associated spectra of W126 in DsbA mutants. Data from [88].

were used to calculate the decay-associated spectra (Figure 17.29). As is usually seen with single-tryptophan proteins, the intensity decays were multi-exponential. The DAS show that Q74 and N127 were responsible for quenching of W126. For the protein containing these residues, W76F, the largest component in the DAS is for a decay time of 0.14 ns. For the protein-lacking residues N127 and Q74 (Figure 17.28, lower panel) the DAS are dominated by a component with a lifetime of 3.57 ns. In examining these data it is important to notice that the individual lifetimes were not assigned to a quenched or unquenched residue. In the quenched mutant protein (Figure 12.29 top) and in the unquenched mutant proteins (bottom) the tryptophan residue displays at least three decay times. The effects of Q74 and N127 were determined by considering which decay times were dominant in the total emission.

17.6.3. Immunophilin FKBP59-I: Quenching of Tryptophan Fluorescence by Phenylalanine

Immunophilin FKBP59-I provides another example of quenching of tryptophan by a nearby amino-acid side chain.[90] In this case the quencher is phenylalanine, which is not usually considered a quencher. Immunophilins are receptors for immunosuppressant drugs such as cyclosporin. The immunophilin domain FKBP59-I contains two tryptophan residues at positions 59 and 89 (Figure 17.30). In general it would be difficult to separate the contributions of the two tryptophan residues using data for just FKBP59-I. An analogous protein FKBP12 was available that contained just W89. The intensity of these two proteins is markedly different, with W89 showing a much lower quantum yield (0.025 versus 0.19 for FKBP59). Trp-89 in FKBP12 shows more rapid intensity decay than FKBP59-I, with two tryptophan residues (Figure 17.31). For the protein with two tryptophan residues, one of which is highly-fluorescent, the lifetime distribution analysis shows a dominant decay time near 6.16 ns. For the single-tryptophan protein the intensity decay is dominated by the more weakly emitting residue, which displays a more heterogeneous intensity decay with a dominant decay time near 0.21 ns

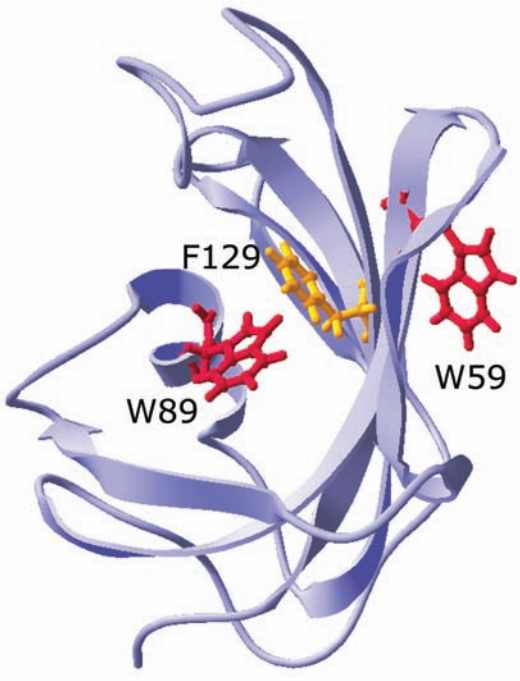

Figure 17.30. Location of the two tryptophan in FKBP59-I. FKBP12 has only trp-89.

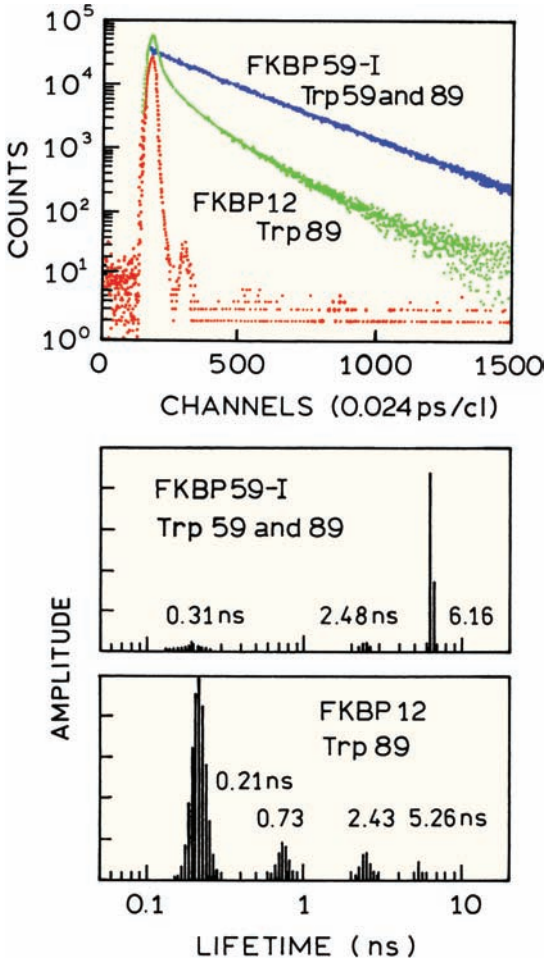

Figure 17.31. **Top**: Time-resolved intensity decay of FKBP59-I and FKBP12. **Bottom**: Lifetime distribution recovered using the maximum entropy method. Excitation at 295 nm. Emission at 340 nm, 20°C. Reprinted with permission from [90]. Copyright © 1997, American Chemical Society.

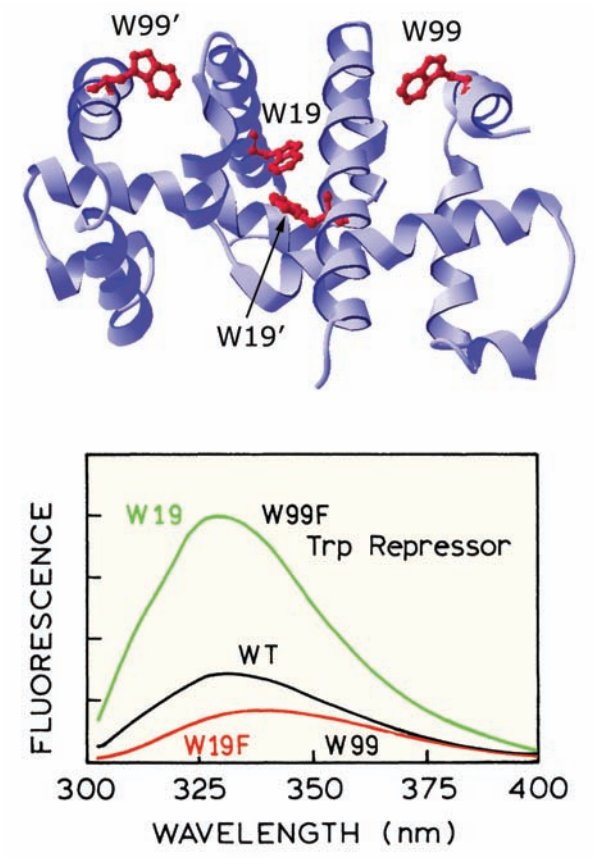

Figure 17.32. Emission spectra of the wild-type *E. coli* trp repressor (WT) and its two single-tryptophan mutants. Revised from [92].

(Figure 17.31, lower panel). These results revealed an unexpected origin for quenching of W89. Apparently this tryptophan residue is quenched due to a nearby phenylalanine residue. Benzene is known to decrease the decay times of indole.[91] Although not reported, one would expect denaturation of the protein to decrease the extent of quenching and normalize the fluorescence of W89, which would support the conclusion that F129 is responsible for quenching of W89.

17.6.4. Trp Repressor: Resolution of the Two Interacting Tryptophans

Site-directed mutagenesis and frequency-domain measurements were used to study the two tryptophan residues in the tryptophan repressor from *E. coli*.[92–93] The wild-type protein is a symmetrical dimer and contains two tryptophans at positions 19 and 99 in each subunit. The W99F mutant contains only tryptophan 19 (W19) and the W19F mutant contains only tryptophan 99 (W99). Emission spectra of the three proteins show that the protein with W19 has a higher quantum yield than the protein with W99, or even the wild-type protein with two tryptophan residues (Figure 17.32).

Frequency-domain intensity decays of the three repressor proteins show that each displays a distinct intensity decay (Figure 17.33). The longest decay time is shown by the mutant with W19, as can be judged by the larger phase angles at lower frequencies. The mean decay time of W19 is even longer than that of the wild-type protein. These results indicate that W99 acts as a quencher in the wild-type protein, presumably by RET from W19 to W99. This is reasonable because W19 has a shorter emission maximum than W99.

The difficulties in resolving the emission from each residue using only the wild-type protein is illustrated by the

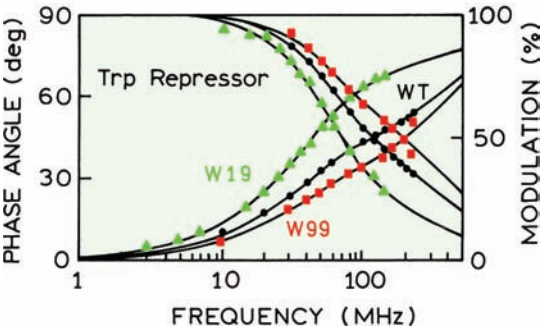

Figure 17.33. Frequency-domain intensity decay of the trp repressor (●) and its two single-tryptophan mutants with W19 (▲) or W99 (■). Revised and reprinted with permission from [92]. Copyright © 1993, American Chemical Society.

intensity decays (Table 17.5). Both the wild-type protein and the single-tryptophan mutants display a double-exponential decay. The decay times overlap for all three proteins. Also, the interactions between the tryptophan residues imply that the intensity decay of the wild-type protein is not a result of adding the intensity decays of the two single-tryptophan mutants. The emission of the wild-type protein is not the sum of the emission of the two single-tryptophan mutants.

17.6.5. Thermophilic β-Glycosidase: A Multi-Tryptophan Protein

In the preceding sections we saw studies of proteins with a limited number of tryptophan residues. As the number of tryptophan residues increases, it becomes impractical to resolve the individual residues. Even if single-tryptophan mutants can be made it is unlikely that the protein will remain stable after substitution of a large number of tryptophan residues. In such cases it can be informative to examine the lifetime distributions of the wild-type protein. *S. solfataricus* is an extreme thermophile growing at 87°C. Its β-glycosidase is a 240-kDa tetramer that contains 68 tryptophan residues, 17 per subunit (Figure 17.34). The β-glycosidase remains native and active to above 85°C. It is impractical to attempt to resolve the individual emission spectra, and equally impractical to prepare single-tryptophan mutants. One can nonetheless measure the intensity decays of the protein, which in this case were measured using the frequency-domain method. The decays are highly heterogeneous and were interpreted in terms of a bimodal lifetime distribution (Figure 17.35). As the temperature is increased the two components shift progressively towards shorter lifetimes.[94]

Table 17.5. Intensity Decays of the Trp Repressor, and Its Single–Tryptophan Mutants[a]

Protein	τ_i (ns)	α_i	f_i	$\bar{\tau}$ (ns)[b]
WT (W19 and W99)	0.57	0.70	0.28	1.41
	3.36	0.30	0.72	
W19F (W99)	0.58	0.83	0.47	1.01
	3.14	0.17	0.53	
W99F (W19)	0.40	0.28	0.04	2.95
	3.94	0.72	0.96	

[a]From [92].
[b]Calculated using $\bar{\tau} = \Sigma_i f_i \tau_i$.

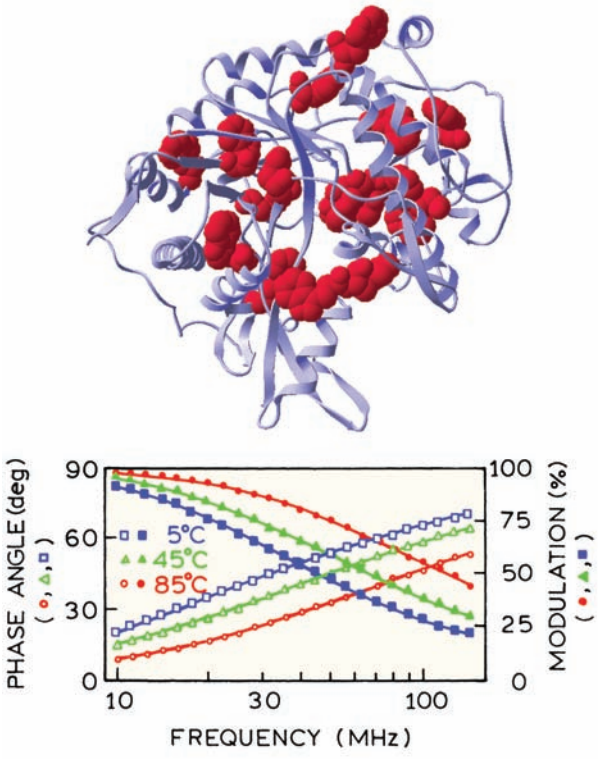

Figure 17.34. Frequency dependence of the phase shift and demodulation factors of *S. solfataricus* β-glycosidase fluorescence emission at neutral pH at 5, 45, and 85°C. The structure is one monomer from the tetramer; tryptophans are in red. Revised from [94].

17.6.6. Heme Proteins Display Useful Intrinsic Fluorescence

For many years it was assumed that heme proteins were nonfluorescent. This was a reasonable assumption given that the intense Soret absorption band of the heme groups is expected to result in Förster distances (R_0) for trp to heme

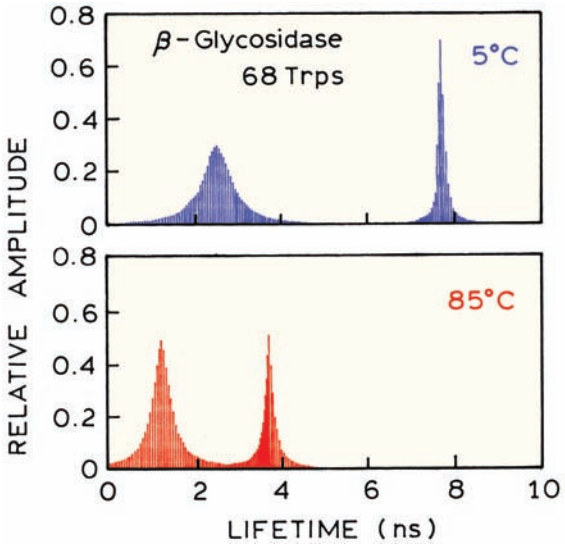

Figure 17.35. Tryptophanyl-lifetime-distribution of *S. solfataricus* β-glycosidase at the indicated temperatures. Revised from [94].

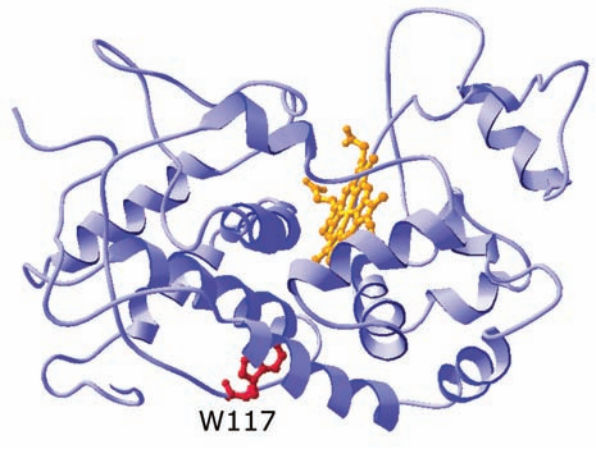

Figure 17.36. Structure of seed-coat soybean peroxidase.

transfer near 32–34 Å. Since this distance is larger than the 20-Å radius of a myoglobin molecule, RET is expected to be nearly complete.

Detection of tryptophan emission from heme proteins is experimentally difficult. Suppose RET quenching is 99% efficient, and suppose that your protein solution contains a 1% impurity of the apoprotein or some non-heme protein. The signal from the impurity will be approximately equal to that from the heme protein. For this reason it is difficult to prove if the observed weak emission is due to heme proteins, to impurities, or to the apoproteins. In spite of these difficulties, some groups were successful in detecting heme protein emission from the steady-state data.[95–98] Subsequent time-resolved experiments confirmed that heme proteins do display weak intrinsic fluorescence, and the ps decay times found in heme proteins can be correlated with their structure.[99–106]

An example of intrinsic fluorescence from a heme protein is provided by seed-coat soybean peroxidase (SBP).[105] This protein contains 326 amino acids and a single-tryptophan residue, W117 (Figure 17.36). The intensity decay of W117 is highly heterogeneous, showing at least four decay times (Figure 17.37). The lifetime distribution recovered from the intensity decay is informative in showing that 97% of the steady-state intensity is due to the 36-ps component. This result illustrates the difficulty in studies of heme protein fluorescence. It is difficult to know if the minor longer lifetime components are due to the heme protein itself, or impurities, apoprotein, or unusual conformations of the heme protein that do not allow efficient energy transfer.

The emission of heme proteins has also been studied using the frequency-domain method.[106] Representative intensity decays for hemoglobin are shown in Figure 17.38.

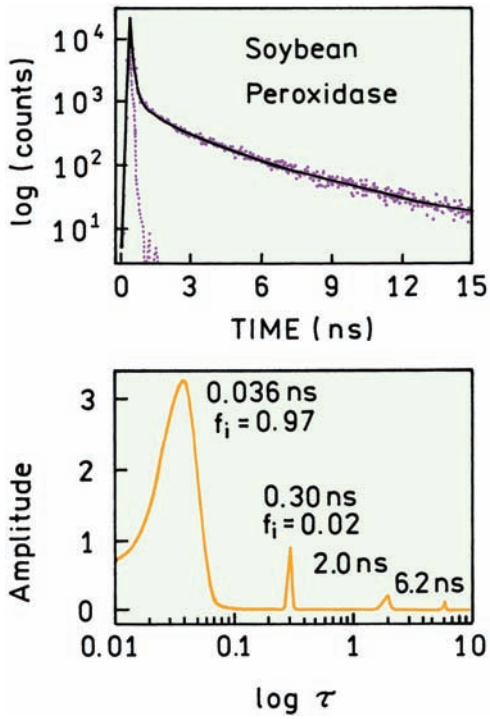

Figure 17.37. Intensity decays of the intrinsic tryptophan emission from soybean peroxidase. The fractional intensities of the 2.0- and 6.2-ns components are near 0.008 and 0.002, respectively. Data from [105].

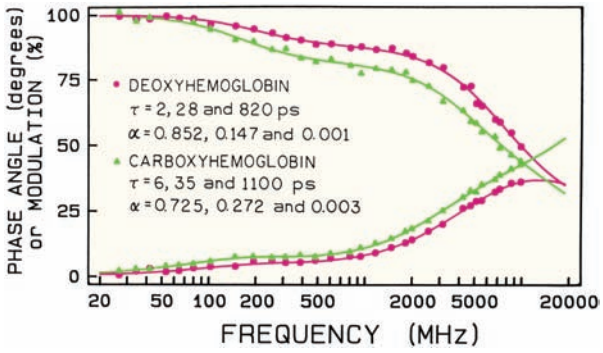

Figure 17.38. Frequency-domain intensity decays of the intrinsic tryptophan fluorescence from hemoglobin. From [106].

The frequency-domain data revealed both ps and ns decay times. Long-lifetime ns components were also found for myoglobin. These long-lived components are thought to be due to conformational isomers of the proteins in which the heme on the tryptophan residue is positioned so that energy transfer cannot occur. The time-resolved data can provide useful information under conditions where the steady-state data are ambiguous.

17.7. TIME-DEPENDENT SPECTRAL RELAXATION OF TRYPTOPHAN Advanced Topic

We have seen many examples of resolving the emission from individual tryptophan residues in multi-tryptophan proteins. During this analysis we assumed that each tryptophan residue displayed the same lifetime at all emission wavelengths. However, the lifetimes of a single-tryptophan residue may not be the same at all emission wavelengths. Many examples are known where the intensity decays are different at different wavelengths. If the intensity decay of indole in water is measured the decays will be essentially the same at all emission wavelengths. However, the decays become strongly dependent on emission wavelength in more viscous solvents. Figure 17.39 shows intensity decay of indole in glycerol at 20°C. The intensity decays were measured for various wavelengths across the emission spectrum.[107] The intensity decay at 310 nm, which is on the blue side of the emission, is more rapid than the decay at 390 nm, which is on the long-wavelength side of the emission. This difference is due to solvent relaxation around the excited state, which is occurring on a timescale comparable to the decay time (Chapter 7). The intensity decay at 380 nm shows a rise time that is proof of an excited-state process.

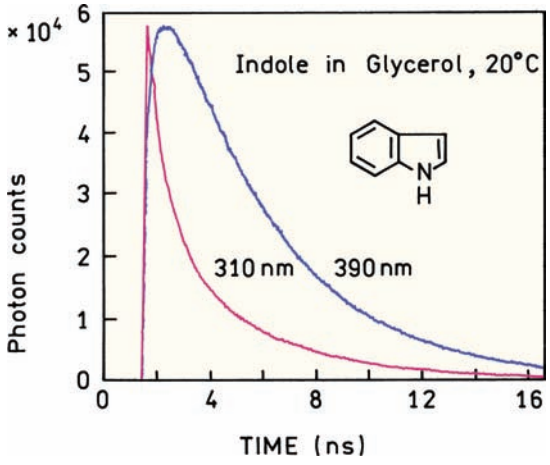

Figure 17.39. Intensity decays of indole in glycerol at 20°C. Revised from [107].

The intensity decays at each wavelength can be analyzed by the multi-exponential model. In this global analysis the lifetimes τ_i were assumed to be independent of wavelength and the amplitude $\alpha_i(\lambda)$ was assumed to depend on wavelength. These are the same assumptions that are commonly used when analyzing wavelength-dependent data from proteins. The wavelength-dependent decays allow calculation of the decay-associated spectra (Figure 17.40, top). The results are presented in wavenumber units. The DAS for shorter decay times show shorter wavelength emission maxima, and the amplitudes are negative at some wavelengths.

For indole in glycerol we do not expect unique emitting species, so the DAS in Figure 17.40 give the misleading impression of discrete emitting states. The recovered decays can also be used to calculate the time-resolved emission spectra (Figure 17.40, bottom). The TRES show a gradual shift to longer wavelengths and probably provide a more reasonable description of indole in glycerol. Time-dependent spectral relaxation can result in DAS that are not due to unique emitting species.

Tryptophan residues in a protein are in a viscous environment, probably comparable to glycerol. A large amount of data suggest that spectral relaxation occurs in many proteins,[108–119] but there may also be proteins where relaxation does not occur. When wavelength-dependent intensity decays are measured for a protein it is not always clear whether to use DAS or TRES. For a multi-tryptophan protein one is tempted to use DAS and to associate the DAS with the individual tryptophan residues. This association may not always be correct. Similarly, for a single-tryptophan protein there is a tendency to associate the DAS with

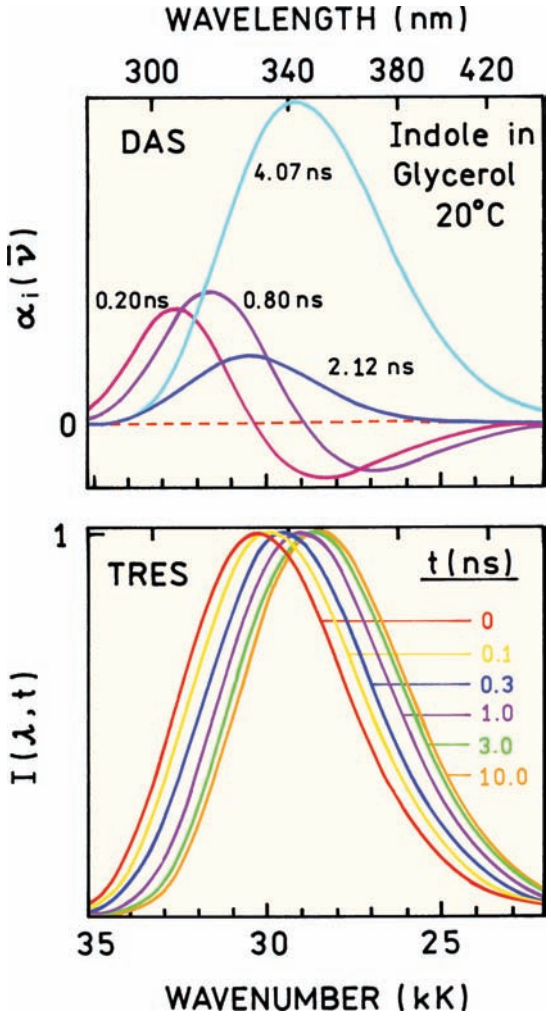

Figure 17.40. Decay-associated spectra (top) and time-resolved emission spectra (bottom). The DAS and TRES were calculated from the same time-resolved decays of indole in glycerol at 20°C. Revised from [107].

multiple conformations. However, it is important to remember that the DAS and TRES are representations of the data, and not of the protein. Most time-resolved data are not adequate to distinguish between discrete DAS or continuous relaxation.

Evidence for time-dependent relaxation of tryptophan residues is pervasive but not specific. One characteristic of spectral relaxation is an increase of the mean decay time with increasing observation wavelength. Since there seems to be no correlation between the emission maxima of proteins and their mean lifetimes (see Figure 16.12), there should be equal numbers of proteins that display increases or decreases in lifetime with increasing wavelength. However, for almost all proteins the mean lifetime increases with increasing emission wavelength, which is characteristic of spectral relaxation. Even single-tryptophan proteins display lifetimes that increase with increasing wavelength. An unambiguous characteristic of an excited-state process is a negative pre-exponential factor in the intensity decay. Such components have only been rarely observed in proteins, one example being chicken pepsinogen.[115] The absence of negative pre-exponential factors does not prove the absence of spectral relaxation because these terms are easily eliminated by spectral overlap. However, the correlation between shorter emission wavelengths and shorter lifetimes could also be due to quenching by peptide bonds.

The difficulty in interpreting the data in terms of DAS or spectral relaxation is illustrated by studies of myelin basic protein (MBP),[119] which contains a single-tryptophan residue. This protein is found in the central nervous system associated with myelin. In solution in the absence of membranes, MBP is thought to be mostly unstructured. Time-resolved decays were collected across the emission spectrum and used to calculate the DAS and TRES (Figure 17.41). The DAS seem to imply multiple conformations and the TRES suggest a continuous relaxation process. The time-resolved data usually do not indicate whether the decays are due to discrete emitting species or a continuously changing population. Most papers on protein fluorescence select either the DAS or TRES for presentation, depending on the preferred interpretation of the data.

Under favorable conditions ground-state heterogeneity or spectral relaxation can be distinguished by detection of a negative pre-exponential factor on the long-wavelength side of the emission. Such a factor is rarely observed for proteins.[115] The typical absence of negative pre-exponential factors in proteins is probably due to the modest spectral shift during the excited-state lifetimes and spectral overlap between the initially excited and relaxed states (Chapter 7). Negative pre-exponential factors can be seen from indole derivatives under conditions that may mimic the interior of proteins.[120–121] Figure 17.42 shows the lifetime distributions for tryptophan octyl ester (TOE) in micelles of an uncharged detergent. On the short-wavelength side (305 nm) the amplitudes are all positive. The amplitudes become negative on the long-wavelength (375 nm) side of the emission, which proves that spectral relaxation has occurred. In proteins the time-dependent spectral shifts are usually smaller, and the multiple-tryptophan residues emit at different wavelengths. These factors probably prevent the appearance of negative pre-exponential factors. For most proteins it is probably safe to assume that multiple-tryptophan

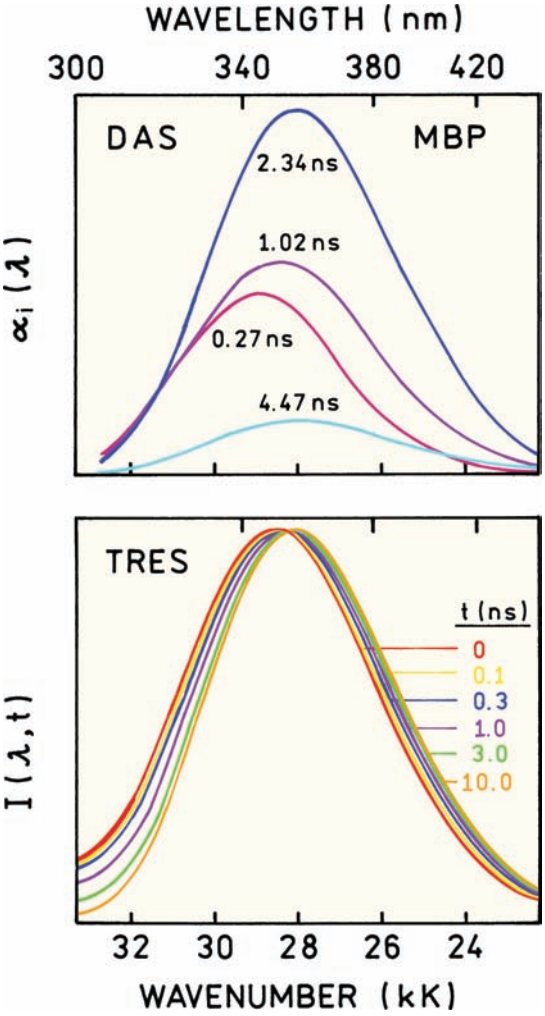

Figure 17.41. Decay-associated spectra and time-resolved emission spectra from myelin basic protein at 30°C, 289-nm excitation. Revised from [119].

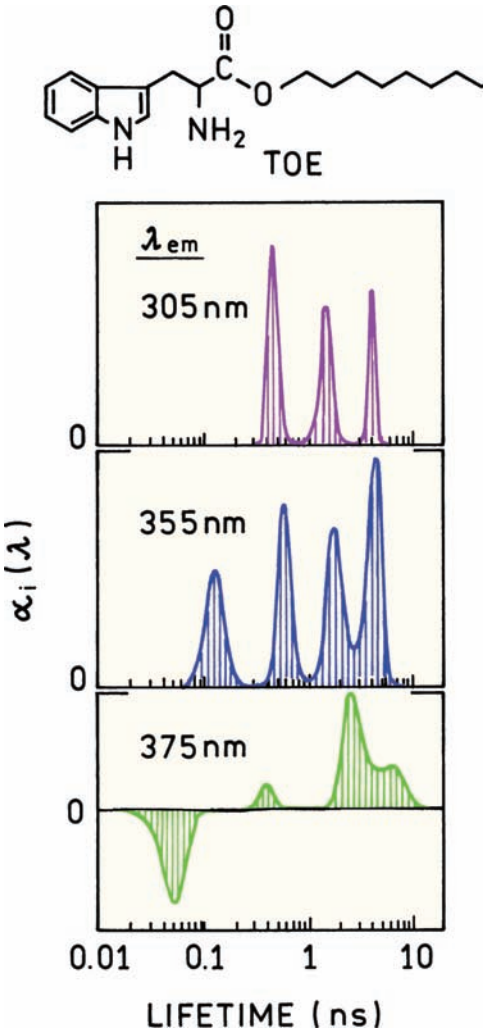

Figure 17.42. Lifetime distributions for tryptophan octyl ester (TOE) in dodecylmaltoside (DM) micelles, 20°C. Revised from [121].

residues, multiple conformations, and spectral relaxation all affect the intensity decays.

17.8. PHOSPHORESCENCE OF PROTEINS

Advanced Topic

Phosphorescence is usually observed at low temperature and/or in the complete absence of quenchers.[122–124] These conditions are needed because phosphorescence lifetimes are typically long—milliseconds to seconds—and thus quenched by low concentrations of oxygen or impurities. Low temperatures are also needed to decrease the rates of non-radiative decay to be comparable with the phosphorescence emission rates. Otherwise, the quantum yield of phosphorescence will be very small.

Figure 17.43 shows the fluorescence and phosphorescence of tryptophan in a glass at low temperatures.[125] Phosphorescence occurs at longer wavelengths than fluorescence, and phosphorescence spectra are typically more structured. The phosphorescence is shown as a separate spectrum from the fluorescence. A separate phosphorescence spectrum is only observed if detection of the phosphorescence is gated to remove the fast decay fluorescence. More typical spectra are shown in Figure 17.44 for NATA in a glass-forming solvent at various temperatures.[126] At low temperature (100 to 190°K) the phosphorescence appears on the long-wavelength side of the fluorescence spectrum. Without gated detection both emissions are observed. The wavelength resolution of the phosphorescence is lower in Figure 17.44 than in Figure 17.43. The

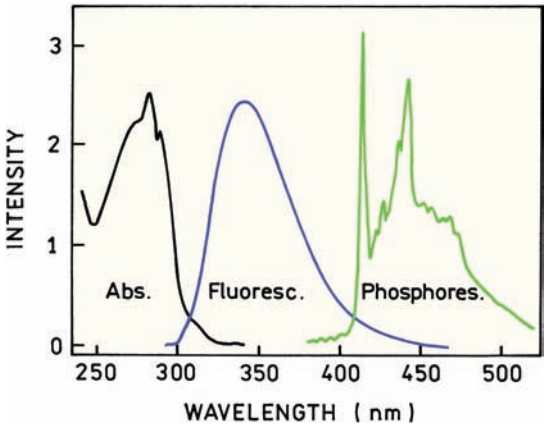

Figure 17.43. Absorption, fluorescence, and phosphorescence spectra of tryptophan in a low-temperature glass. Revised from [125].

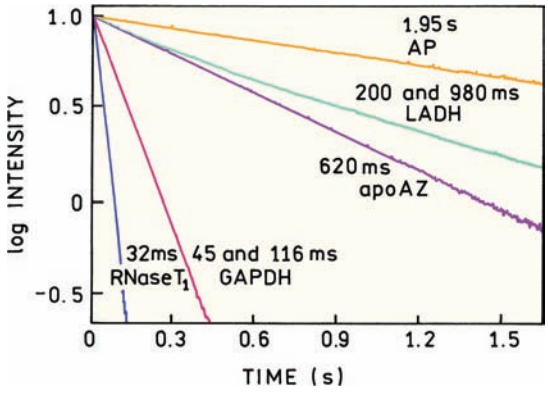

Figure 17.45. Phosphorescence intensity decays of proteins in aqueous solution at room temperature. Revised from [140].

spectra in 17.44 are more typical because a bandpass near 5 nm is typically used in recording fluorescence spectra. If the decay times were measured at 350 and 450 nm, the 450-nm emission would show a millisecond decay time and the 350-nm emission the usual nanosecond decay time.

In the 1980 reports there appeared an observation of tryptophan phosphorescence from proteins at room temperature,[127–129] in some cases in the presence of oxygen.[130] This was surprising given the long lifetimes for phosphorescence. Some of the early reports were in error due to depletion of oxygen with intense excitation intensities.[131] In spite of this initial confusion it is now accepted that some proteins display phosphorescence in solution at room temperature.[132–140] Observation of useful phosphorescence requires the complete exclusion of oxygen, but some studies have been performed with oxygen concentrations up to about 80 μM.

The phosphorescence decay times of proteins at room temperature can be surprisingly long (Figure 17.45).[140] In contrast to fluorescence decays the decays of phosphorescence seem to be more like single exponentials. Buried tryptophans with short emission wavelength tend to have longer phosphorescence decay times than exposed residues (Table 17.6).[141] The nearly single-exponential decays of phosphorescence and the large range of phosphorescence decay times suggest the possibility of resolving the emission of several tryptophans in a multi-tryptophan protein.

The highly structured emission of tryptophan phosphorescence can allow the resolution of two tryptophan residues in a single protein.[92] This possibility is shown for the tryptophan repressor and its single-tryptophan mutants

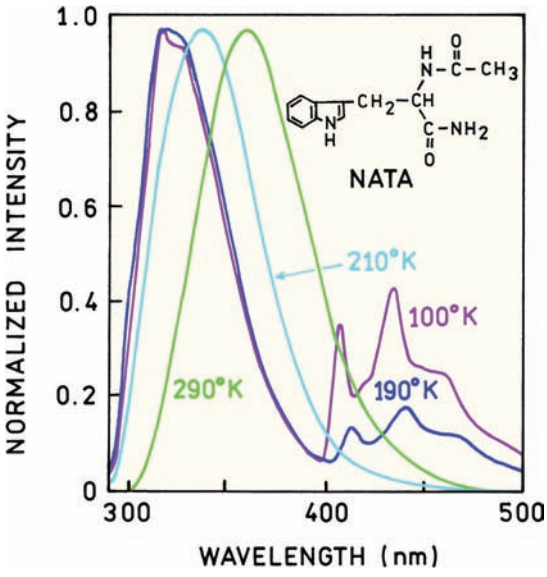

Figure 17.44. Emission spectra of NATA in a glycerol–water mixture. Revised from [126].

Table 17.6. Correlation of Fluorescence Emission Maximum and Phosphorescence Lifetime in Single-Tryptophan Proteins[a]

Protein	Fluorescence maximum (nm)	Phosphorescence lifetime (ms)
Azurin	305	400
Parvalbumin (calcium)	320	5
Ribonuclease T_1	325	14
Melittin	340	<0.5
Monellin	345	<0.5
Parvalbumin (no calcium)	350	<0.5

[a]From [141].

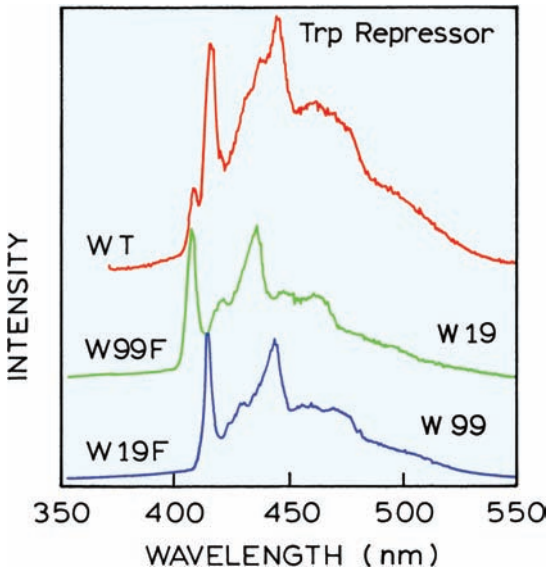

Figure 17.46. Low-temperature phosphorescence spectra of wild-type (WT) trp repressor and its two single-tryptophan mutants at liquid nitrogen temperature. The spectra are offset for visualization. Revised from [92].

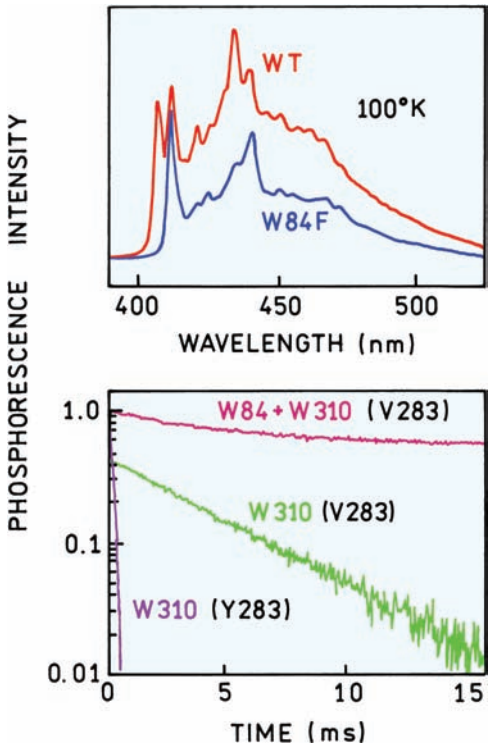

Figure 17.47. **Top**: Phosphorescence emission spectra of wild-type glyceraldehyde-3-phosphate dehydrogenase (GPD) and its W84F mutant at 100°K. **Bottom**: Phosphorescence intensity decays of mutants of GPD at 0°C. The letters and numbers in parentheses refer to the residues present in the mutant protein. Revised from [146].

(Figure 17.46). The wild-type protein shows two sharp peaks near 400 nm, and each of the single-tryptophan mutants show a single peak near this wavelength. Each of these peaks is thus due to a single-tryptophan residue.

Multiple phosphorescence peaks have been observed for other proteins with two tryptophan residues.[142–145] Site-directed mutagenesis has been used to identify amino-acid side chains that quench tryptophan phosphorescence.[146] Figure 17.47 shows the phosphorescence emission spectra of glyceraldehyde-3-phosphate dehydrogenase (GPD) from *Bacillus stearothermophilus*. The wild-type protein contains two tryptophan residues: W84 and W310. The emission spectrum of the W84F mutant allows assignment of the peaks near 400 nm to each tryptophans residue. The lower panel shows the phosphorescence decays at 0°C. The mutant containing W310 shows a very short phosphorescence decay time. This short decay time is due to a tyrosine residue at position 283 (Y283). Replacement of this tyrosine with a valine (V) results in a 50-fold increase in the decay time of W310.

17.9. PERSPECTIVES ON PROTEIN FLUORESCENCE

Our understanding of protein fluorescence has increased dramatically in the past five years. The availability of a large number of protein structures allows correlation between structural features of the proteins and their spectral properties. General trends are beginning to emerge, such as which side chains are most likely to quench tryptophan. Energy transfer from short- to long-wavelength tryptophans has been seen for several proteins. Emission maxima can be correlated with exposure to solvent, as seen from the protein structure. This improved understanding of protein fluorescence will allow its use to answer more specific questions about protein function and protein interactions with other biomolecules.

REFERENCES

1. Birch DJS, Imhof RE. 1991. Time-domain fluorescence spectroscopy using time-correlated single-photon counting. In *Topics in fluorescence spectroscopy*, Vol. 1: *Techniques*, pp. 1–95. Ed JR Lakowicz. Plenum Press, New York.
2. Lakowicz JR, Gryczynski I. 1991. Frequency-domain fluorescence spectroscopy. In *Topics in fluorescence spectroscopy*, Vol 1: *Techniques*, pp. 293–355. Ed JR Lakowicz. Plenum Press, New York.

3. Grinvald A, Steinberg IZ. 1976. The fluorescence decay of tryptophan residues in native and denatured proteins. *Biochim Biophys Acta* **427**:663–678.
4. Beechem JM, Brand L. 1985. Time-resolved fluorescence of proteins. *Annu Rev Biochem* **54**:43–71.
5. Rayner DM, Szabo AG. 1978. Time-resolved fluorescence of aqueous tryptophan. *Can J Chem* **56**:743–745.
6. Szabo AG, Rayner DM. 1980. Fluorescence decay of tryptophan conformers in aqueous solution. *J Am Chem Soc* **102**:554–563.
7. Gudgin E, Lopez-Delgado R, Ware WR. 1981. The tryptophan fluorescence lifetime puzzle: a study of decay times in aqueous solution as a function of pH and buffer composition. *Can J Chem* **59**:1037–1044.
8. McLaughlin ML, Barkley MD. 1997. Time-resolved fluorescence of constrained tryptophan derivatives: implications for protein fluorescence. *Methods Enzymol* **278**:190–202.
9. Schiller PW. 1985. Application of fluorescence techniques in studies of peptide conformations and interactions. *Peptides* **7**:115–164.
10. Robbins RJ, Fleming GR, Beddard GS, Robinson GW, Thistlethwaite PJ, Woolfe GJ. 1980. Photophysics of aqueous tryptophan: pH and temperature effects. *J Am Chem Soc* **102**:6271–6280.
11. Eftink MR, Jia Y, Hu D, Ghiron CA. 1995. Fluorescence studies with tryptophan analogues: excited state interactions involving the side chain amino group. *J Phys Chem* **99**:5713–5723.
12. Petrich JW, Chang MC, McDonald DB, Fleming GR. 1983. On the origin of nonexponential fluorescence decay in tryptophan and its derivatives. *J Am Chem Soc* 105:3824–3832.
13. Chen Y, Liu B, Yu H-T, Barkley MD. 1996. The peptide bond quenches indole fluorescence. *J Am Chem Soc* **118**(39):9271–9278.
14. Chen Y, Liu B, Barkley MD. 1995. Trifluoroethanol quenches indole fluorescence by excited-state proton transfer. *J Am Chem Soc* **117**:5608–5609.
15. Steiner RF, Kirby EP. 1969. The interaction of the ground and excited states of indole derivatives with electron scavengers. *J Phys Chem* **15**:4130–4135.
16. Froehlich PM, Gantt D, Paramasigamani V. 1977. Fluorescence quenching of indoles by N,N-dimethylformamide. *Photochem Photobiol* **26**:639–642.
17. Ricci RW, Nesta JM. 1976. Inter- and intramolecular quenching of indole fluorescence by carbonyl compounds. *J Phys Chem* **80**(9): 974–980.
18. Shopova M, Genov N. 1983. Protonated form of histidine 238 quenches the fluorescence of tryptophan 241 in subtilisin novo. *Int J Pept Protein Res* **21**:475–478.
19. Butler J, Land EJ, Prutz WA, Swallow AJ. 1982. Charge transfer between tryptophan and tyrosine in proteins. *Biochim Biophys Acta* **705**:150–162.
20. Prutz WA, Siebert F, Butler J, Land EJ, Menez A, Montenay-Garestier T. 1982. Intramolecular radical transformations involving methionine, tryptophan and tyrosine. *Biochim Biophys Acta* **705**:139–149.
21. Sanyal G, Kim E, Thompson FM, Brady EK. 1989. Static quenching of tryptophan fluorescence by oxidized dithiothreitol. *Biochem Biophys Res Commun* **165**(2):772–781.
22. Eftink MR. 1991. Fluorescence quenching reactions. In *Biophysical and biochemical aspects of fluorescence spectroscopy*, pp. 1–41. Ed TG Dewey. Plenum Press, New York.
23. Adams P, Chen Y, Ma K, Zagorski M, Sonnichsen FD, McLaughlin ML. 2002. Intramolecular quenching of tryptophan fluorescence by the peptide bond in cyclic hexapeptides. *J Am Chem Soc* **124**:9278–9286.
24. Chen Y, Barkley MD. 1998. Toward understanding tryptophan fluorescence in proteins. *Biochemistry* **37**:9976–9982.
25. Jameson DM, Weber G. 1981. Resolution of the pH-dependent heterogeneous fluorescence decay of tryptophan by phase and modulation measurements. *J Phys Chem* **85**:953–958.
26. Chen RF, Knutson JR, Ziffer H, Porter D. 1991. Fluorescence of tryptophan dipeptides: correlations with the rotamer model. *Biochemistry* **30**:5184–5195.
27. Shizuka H, Serizawa M, Shimo T, Saito I, Matsuura T. 1988. Fluorescence-quenching mechanism of tryptophan: remarkably efficient internal proton-induced quenching and charge-transfer quenching. *J Am Chem Soc* **110**:1930–1934.
28. Callis PR, Liu T. 2004. Quantitative prediction of fluorescence quantum yields for tryptophan in proteins. *J Phys Chem B* **108**:4248–4259.
29. Malak H, Gryczynski I, Lakowicz JR. Unpublished observations.
30. Lakowicz JR, Jayaweera R, Szmacinski H, Wiczk W. 1989. Resolution of two emission spectra for tryptophan using frequency-domain phase-modulation spectra. *Photochem Photobiol* **50**(4): 541–546.
31. Ruggiero AJ, Todd DC, Fleming GR. 1990. Subpicosecond fluorescence anisotropy studies of tryptophan in water. *J Am Chem Soc* **112**: 1003–1014.
32. Döring K, Konermann L, Surrey T, Jähnig F. 1995. A long lifetime component in the tryptophan fluorescence of some proteins. *Eur Biophys J* **23**:423–432.
33. Lakowicz JR, Laczko G, Gryczynski I. 1987. Picosecond resolution of tyrosine fluorescence and anisotropy decays by 2-GHz frequency-domain fluorometry. *Biochemistry* **26**:82–90.
34. Ross JBA, Laws WR, Rousslang KW, Wyssbrod HR. 1992. Tyrosine fluorescence and phosphorescence from proteins and polypeptides. In *Topics in fluorescence spectroscopy*, Vol. 3: *Biochemical applications*, pp. 1–63. Ed JR Lakowicz. Plenum Press, New York.
35. Laws WR, Ross JBA, Wyssbrod HR, Beechem JM, Brand L, Sutherland JC. 1986. Time-resolved fluorescence and ^{1}H NMR studies of tyrosine and tyrosine analogues: correlation of NMR-determined rotamer populations and fluorescence kinetics. *Biochemistry* **25**:599–607.
36. Ross JBA, Laws WR, Sutherland JC, Buku A, Katsoyannis PG, Schwartz IL, Wysobrod HR. 1986. Linked-function analysis of fluorescence decay functions: resolution of side-chain rotamer populations of a single aromatic amino acid in small polypeptides. *Photochem Photobiol* **44**:365–370.
37. Contino PB, Laws WR. 1991. Rotamer-specific fluorescence quenching in tyrosinamide: dynamic and static interactions. *J Fluoresc* **1**(1):5–13.
38. Noronha M, Lima JC, Lamosa P, Santos H, Maycock C, Ventura R, Maçanita AL. 2004. Intramolecular fluorescence quenching of tyrosine by the peptide α-carbonyl group revisited. *J Phys Chem A* **108**: 2155–2166.
39. Seidel C, Orth A, Greulich K-O. 1993. Electronic effects on the fluorescence of tyrosine in small peptides. *Photochem Photobiol* **58**(2): 178–184.

40. Leroy E, Lami H, Laustriat G. 1971. Fluorescence lifetime and quantum yield of phenylalanine aqueous solutions: temperature and concentration effects. *Photochem Photobiol* **13**:411–421.
41. Sudhakar K, Wright WW, Williams SA, Phillips CM, Vanderkooi JM. 1993. Phenylalanine fluorescence and phosphorescence used as a probe of conformation for cod parvalbumin. *J Fluoresc* **3**(2):57–64.
42. Lankiewicz L, Stachowiak K, Rzeska A, Wiczk W. 1999. Photophysics of sterically constrained peptides. In *Peptide science—present and future*, pp. 168–170. Ed Y Shimonishi. Kluwer, London.
43. Guzow K, Ganzynkowicz R, Rzeska A, Mrozek J, Szabelski M, Karolczak J, Liwo A, Wiczk W. 2004. Photophysical properties of tyrosine and its simple derivatives studied by time-resolved fluorescence spectroscopy, global analysis, and theoretical calculations. *J Phys Chem B* **108**:3879–3889.
44. Tanaka F, Tamai N, Mataga N, Tonomura B, Hiromi K. 1994. Analysis of internal motion of single tryptophan in *Streptomyces* subtilisin inhibitor from its picosecond time-resolved fluorescence. *Biophys J* **67**:874–880.
45. Tanaka F, Mataga N. 1992. Non-exponential decay of fluorescence of tryptophan and its motion in proteins. In *Dynamics and mechanisms of photoinduced electron transfer and related phenomena*, pp. 501–512. Ed N Mataga, T Okada, H Masuhara. North-Holland, Amsterdam.
46. Eftink MR, Ghiron CA, Kautz RA, Fox RO. 1989. Fluorescence lifetime studies with staphylococcal nuclease and its site-directed mutant: test of the hypothesis that proline isomerism is the basis for nonexponential decays. *Biophys J* **55**:575–579.
47. Dahms TES, Willis KJ, Szabo AG. 1995. Conformational heterogeneity of tryptophan in a protein crystal. *J Am Chem Soc* **117**: 2321–2326.
48. Tanaka F, Mataga N. 1987. Fluorescence quenching dynamics of tryptophan in proteins. *Biophys J* **51**:487–495.
49. Alcala JR. 1994. The effect of harmonic conformational trajectories on protein fluorescence and lifetime distributions. *J Chem Phys* **101**(6):4578–4584.
50. Eftink MR, Ghiron CA. 1975. Dynamics of a protein matrix as revealed by fluorescence quenching. *Proc Natl Acad Sci USA* **72**: 3290–3294.
51. Eftink MR, Ghiron CA. 1977. Exposure of tryptophanyl residues and protein dynamics. *Biochemistry* **16**:5546–5551.
52. Eftink MR, Hagaman KA. 1986. The viscosity dependence of the acrylamide quenching of the buried tryptophan residue in parvalbumin and ribonuclease T_1. *Biophys Chem* **25**:277–282.
53. Longworth JW. 1968. Excited state interactions in macromolecules. *Photochem Photobiol* **7**:587–594.
54. James DR, Demmer DR, Steer RP, Verrall RE. 1985. Fluorescence lifetime quenching and anisotropy studies of ribonuclease T_1. *Biochemistry* **24**:5517–5526.
55. Gryczynski I, Eftink M, Lakowicz JR. 1988. Conformation heterogeneity in proteins as an origin of heterogeneous fluorescence decays, illustrated by native and denatured ribonuclease T_1. *Biochim Biophys Acta* **954**:244–252.
56. Eftink MR, Ghiron CA. 1987. Frequency domain measurements of the fluorescence lifetime of ribonuclease T_1. *Biophys J* **52**:467–473.
57. Chen LX-Q, Longworth JW, Fleming GR. 1987. Picosecond time-resolved fluorescence of ribonuclease T_1. *Biophys J* **51**:865–873.
58. Concha NO, Head JF, Kaetzel MA, Dedman JR, Seaton BA. 1993. Rat annexin V crystal structure: Ca^{2+}–induced conformational changes. *Science* **261**:1321-1324.
59. Sopkova J, Gallay J, Vincent M, Pancoska P, Lewit-Bentley A. 1994. The dynamic behavior of Annexin V as a function of calcium ion binding: a circular dichroism, UV absorption, and steady state and time-resolved fluorescence study. *Biochemistry* **33**(15):4490–4499.
60. Sopkova J, Vincent M, Takahashi M, Lewit-Bentley A, Gallay J. 1998. Conformational flexibility of domain III of annexin V studied by fluorescence of tryptophan 187 and circular dichroism: the effect of pH. *Biochemistry* **37**:11962–11970.
61. Toptygin D, Savtchenko RS, Meadow ND, Brand L. 2001. Homogeneous spectrally- and time-resolved fluorescence emission from single-tryptophan mutants of IIA^{Glc} protein. *J Phys Chem B* **105**:2043–2055.
62. Gryczynski I, Lakowicz JR. Unpublished observations.
63. Nishimoto E, Yamashita S, Szabo AG, Imoto T. 1998. Internal motion of lysozyme studied by time-resolved fluorescence depolarization of tryptophan residues. *Biochemistry* **37**:5599–5607.
64. Poveda JA, Prieto M, Encinar JA, Gonzalez-Ros JM, Mateo CR. 2003. Intrinsic tyrosine fluorescence as a tool to study the interaction of the shaker B "ball" peptide with anionic membranes. *Biochemistry* **42**:7124–7132.
65. Damberg P, Jarvet J, Allard P, Mets U, Rigler R, Gräslund A. 2002. ^{13}C–^{1}H NMR relaxation and fluorescence anisotropy decay study of tyrosine dynamics in motilin. *Biophys J* **83**:2812–2825.
66. Kroes SJ, Canters GW, Gilardi G, van Hoek A, Visser AJWG. 1998. Time-resolved fluorescence study of azurin variants: conformational heterogeneity and tryptophan mobility. *Biophys J* **75**:2441–2450.
67. Tcherkasskaya O, Ptitsyn OB, Knutson JR. 2000. Nanosecond dynamics of tryptophans in different conformational states of apomyoglobin proteins. *Biochemistry* **39**:1879–1889.
68. Lakshmikanth GS, Krishnamoorthy G. 1999. Solvent-exposed tryptophans probe the dynamics at protein surfaces. *Biophys J* **77**:1100–1106.
69. Kouyama I, Kinosita K, Ikegami A. 1989. Correlation between internal motion and emission kinetics of tryptophan residues in proteins. *Eur J Biochem* **182**:517–521.
70. Hansen JE, Rosenthal SJ, Fleming GR. 1992. Subpicosecond fluorescence depolarization studies of tryptophan and tryptophanyl residues of proteins. *J Phys Chem* **96**:3034–3040.
71. Ross JBA, Rousslang KW, Brand L. 1981. Time-resolved fluorescence and anisotropy decay of the tryptophan in adrenocorticotropin-(1-24). *Biochemistry* **20**:4361–4369.
72. Nordlund TM, Podolski DA. 1983. Streak camera measurement of tryptophan and rhodamine motions with picosecond time resolution. *Photochem Photobiol* **38**(6):665–669.
73. Nordlund TM, Liu X-Y, Sommer JH. 1986. Fluorescence polarization decay of tyrosine in lima bean trypsin inhibitor. *Proc Natl Acad Sci USA* **83**:8977–8981.
74. Data courtesy of Dr. John Lee, University of Georgia.
75. Liao R, Wang C-K, Cheung HC. 1992. Time-resolved tryptophan emission study of cardiac troponin I. *Biophys J* **63**:986–995.
76. Dittes K, Gakamsky DM, Haran G, Haas E, Ojcius DM, Kourilsky P, Pecht I. 1994. Picosecond fluorescence spectroscopy of a single-chain class I major histocompatibility complex encoded protein in its peptide loaded and unloaded states. *Immunol Lett* **40**:125–132.

77. Lakowicz JR, Gryczynski I, Szmacinski H, Cherek H, Joshi N. 1991. Anisotropy decays of single tryptophan proteins measured by GHz frequency-domain fluorometry with collisional quenching. *Eur Biophys J* **19**:125–140.
78. Lakowicz JR, Cherek H, Gryczynski I, Joshi N, Johnson ML. 1987. Enhanced resolution of fluorescence anisotropy decays by simultaneous analysis of progressively quenched samples. *Biophys J* **51**:755–768.
79. Gryczynski I, Lakowicz JR. Unpublished observations.
80. John E, Jähnig F. 1988. Dynamics of melittin in water and membranes as determined by fluorescence anisotropy decay. *Biophys J* **54**:817–827.
81. Lakowicz JR, Gryczynski I, Cherek H, Laczko G. 1991. Anisotropy decays of indole, melittin monomer and melittin tetramer by frequency-domain fluorometry and multi-wavelength global analysis. *Biophys Chem* **39**:241–251.
82. Georghiou S, Thompson M, Mukhopadhyay AK. 1981. Melittin-phospholipid interaction evidence for melittin aggregation. *Biochim Biophys Acta* **642**:429–432.
83. Dufourcq J, Faucon J-F. 1977. Intrinsic fluorescence study of lipid–protein interactions in membrane models. *Biochim Biophys Acta* **467**:1–11.
84. Faucon JF, Dufourcq J, Lussan C. 1979. The self-association of melittin and its binding to lipids. *FEBS Lett* **102**(1):187–190.
85. Kaszycki P, Wasylewski Z. 1990. Fluorescence-quenching-resolved spectra of melittin in lipid bilayers. *Biochim Biophys Acta* **1040**: 337–345.
86. Papenhuijzen J, Visser AJWG. 1983. Simulation of convoluted and exact emission anisotropy decay profiles. *Biophys Chem* **17**:57–65.
87. De Beuckeleer K, Volckaert G, Engelborghs Y. 1999. Time resolved fluorescence and phosphorescence properties of the individual tryptophan residues of barnase: evidence for protein–protein interactions. *Proteins: Struct Funct Genet* **36**:42–53.
88. Sillen A, Hennecke J, Roethlisberger D, Glockshuber R, Engelborghs Y. 1999. Fluorescence quenching in the DsbA protein from *escherichia coli*: complete picture of the excited-state energy pathway and evidence for the reshuffling dynamics of the microstates of tryptophan. *Proteins: Struct Funct Genet* **37**:253–263.
89. Hennecke J, Sillen A, Huber-Wunderlich M, Engelborghs Y, Glockshuber R. 1997. Quenching of tryptophan fluorescence by the active-site disulfide bridge in the DsbA protein from *escherichia coli*. *Biochemistry* **36**:6391–6400.
90. Rouviere N, Vincent M, Craescu CT, Gallay J. 1997. Immunosuppressor binding to the immunophilin FKBP59 affects the local structural dynamics of a surface β-strand: time-resolved fluorescence study. *Biochemistry* **36**:7339–7352.
91. Suwaliyan A, Klein UKA. 1989. Picosecond study of solute–solvent interaction of the excited state of indole. *Chem Phys Lett* **159**(2–3): 244–250.
92. Eftink MR, Ramsay GD, Burns L, Maki AH, Mann CJ, Matthews CR, Ghiron CA. 1993. Luminescence studies of trp repressor and its single-tryptophan mutants. *Biochemistry* **32**:9189–9198.
93. Royer CA. 1992. Investigation of the structural determinants of the intrinsic fluorescence emission of the trp repressor using single tryptophan mutants. *Biophys J* **63**:741–750.
94. Bismuto E, Irace G, D'Auria S, Rossi M, Nucci R. 1997. Multitryptophan-fluorescence emission decay of β-glycosidase from the extremely thermophilic archaeon *Sulfolobus solfataricus*. *Eur J Biochem* **244**:53–58.
95. Hirsch RE, Nagel RL. 1981. Conformational studies of hemoglobins using intrinsic fluorescence measurements. *J Biol Chem* **256**(3): 1080–1083.
96. Hirsch RE, Peisach J. 1986. A comparison of the intrinsic fluorescence of red kangaroo, horse and sperm whale metmyoglobins. *Biochim Biophys Acta* **872**:147–153.
97. Hirsch RE, Noble RW. 1987. Intrinsic fluorescence of carp hemoglobin: a study of the R6T transition. *Biochim Biophys Acta* **914**: 213–219.
98. Sebban P, Coppey M, Alpert B, Lindqvist L, Jameson DM. 1980. Fluorescence properties of porphyrin-globin from human hemoglobin. *Photochem Photobiol* **32**:727–731.
99. Hochstrasser RM, Negus DK. 1984. Picosecond fluorescence decay of tryptophans in myoglobin. *Proc Natl Acad Sci USA* **81**: 4399–4403.
100. Bismuto E, Irace G, Gratton E. 1989. Multiple conformational states in myoglobin revealed by frequency domain fluorometry. *Biochemistry* **28**:1508–1512.
101. Willis KJ, Szabo AG, Zuker M, Ridgeway JM, Alpert B. 1990. Fluorescence decay kinetics of the tryptophyl residues of myoglobin: effect of heme ligation and evidence for discrete lifetime components. *Biochemistry* **29**:5270–5275.
102. Gryczynski Z, Lubkowski J, Bucci E. 1995. Heme–protein interactions in horse heart myoglobin at neutral pH and exposed to acid investigated by time-resolved fluorescence in the pico- to nanosecond time range. *J Biol Chem* **270**(33):19232–19237.
103. Janes SM, Holtom G, Ascenzi P, Brundri M, Hochstrasser RM. 1987. Fluorescence and energy transfer of tryptophans in *Aplysia* myoglobin. *Biophys J* **51**:653–660.
104. Szabo AG, Krajcarski D, Zuker M, Alpert B. 1984. Conformational heterogeneity in hemoglobin as determined by picosecond fluorescence decay measurements of the tryptophan residues. *Chem Phys Lett* **108**:145–149.
105. Kamal JKA, Behere DV. 2001. Steady-state and picosecond time-resolved fluorescence studies on native and apo seed coat soybean peroxidase. *Biochem Biophys Res Comm* **289**:427–433.
106. Bucci E, Gryczynski Z, Fronticelli C, Gryczynski I, Lakowicz JR. 1992. Fluorescence intensity and anisotropy decays of the intrinsic tryptophan emission of hemoglobin measured with a 10-GHz fluorometer using front-face geometry on a free liquid surface. *J Fluoresc* **2**(1):29–36.
107. Toptygin D, Brand L. 2000. Spectrally- and time-resolved fluorescence emission of indole during solvent relaxation: a quantitative model. *Chem Phys Lett* **322**:496–502.
108. Lakowicz JR. 2000. On spectral relaxation in proteins. *Photochem Photobiol* **72**(4):421–437.
109. Vincent M, Gilles AM, Li de la Sierra IM, Briozzo P, Barzu O, Gallay J. 2000. Nanosecond fluorescence dynamic stokes shift of tryptophan in a protein matrix. *J Phys Chem B* **104**:11286–11295.
110. Zhong D, Pal SK, Zhang D, Chan SI, Zewail AH. 2002. Femtosecond dynamics of rubredoxin: tryptophan solvation and resonance energy transfer in the protein. *Proc Natl Acad Sci USA* **99**(1):13–18.
111. Petushkov VN, van Stokkum IHM, Gobets B, van Mourik F, Lee J, van Grondelle R, Visser AJWG. 2003. Ultrafast fluorescence relaxation spectroscopy of 6,7-dimethyl-(8-ribityl)-lumazine and

riboflavin, free and bound to antenna proteins from bioluminescent bacteria. *J Phys Chem B* **107**:10934–10939.
112. Kamal JKA, Zhao L, Zewail AH. 2004. Ultrafast hydration dynamics in protein unfolding: human serum albumin. *Proc Natl Acad Sci USA* **101**(37):13411–13416.
113. Lakowicz JR, Cherek H. 1980. Nanosecond dipolar relaxation in proteins observed by wavelength-resolved lifetimes of tryptophan fluorescence. *J Biol Chem* **255**:831–834.
114. Demchenko AP, Gryczynski I, Gryczynski Z, Wiczk W, Malak H, Fishman M. 1993. Intramolecular dynamics in the environment of the single tryptophan residue in staphylococcal nuclease. *Biophys Chem* **48**:39–48.
114. Pierce DW, Boxer SG. 1992. Dielectric relaxation in a protein matrix. *J Phys Chem* **96**:5560–5566.
115. Grinvald A, Steinberg IZ. 1974. Fast relaxation process in a protein revealed by the decay kinetics of tryptophan fluorescence. *Biochemistry* **25**(13):5170–5178.
116. Georghiou S, Thompson M, Mukhopadhyay AK. 1982. Melittin–phospholipid interaction studied by employing the single tryptophan residue as an intrinsic fluorescent probe. *Biochim Biophys Acta* **688**:441–452.
117. Szmacinski H, Lakowicz JR, Johnson M. 1988. Time-resolved emission spectra of tryptophan and proteins from frequency-domain fluorescence spectroscopy. *SPIE Proc* **909**:293–298.
118. Buzady A, Erostyak J, Somogyi B. 2000. Phase-fluorimetry study on dielectric relaxation of human serum albumin. *Biophys Chem* **88**: 153–163.
119. Russo AT, Brand L. 1999. A nanosecond time-resolved fluorescence study of recombinant human myelin basic protein. *J Fluoresc* **9**(4): 333–342.
120. Vincent M, Gallay J, Demchenko AP. 1995. Solvent relaxation around the excited state of indole: analysis of fluorescence lifetime distributions and time-dependence spectral shifts. *J Phys Chem* **99**: 14931–14941.
121. De Foresta B, Gallay J, Sopkova J, Champeil P, Vincent M. 1999. Tryptophan octyl ester in detergent micelles of dodecylmaltoside: fluorescence properties and quenching by brominated detergent analogs. *Biophys J* **77**:3071–3084.
122. Steiner RF, Kolinski R. 1968. The phosphorescence of oligopeptides containing tryptophan and tyrosine. *Biochemistry* **7**:1014–1018.
123. Purkey RM, Galley WC. 1970. Phosphorescence studies of environmental heterogeneity for tryptophyl residues in proteins. *Biochemistry* **9**:3569–3575.
124. Strambini GB, Gonnelli M. 1985. The indole nucleus triplet-state lifetime and its dependence on solvent microviscosity. *Chem Phys Lett* **115**(2):196–200.
125. Cioni P, Strambini GB. 2002. Tryptophan phosphorescence and pressure effects on protein structure. *Biochim Biophys Acta* **1595**: 116–130.
126. Wright WW, Guffanti GT, Vanderkooi JM. 2003. Protein in sugar films and in glycerol/water as examined by infrared spectroscopy and by the fluorescence and phosphorescence of tryptophan. *Biophys J* **85**:1980–1995.
127. Kai Y, Imakubo K. 1979. Temperature dependence of the phosphorescence lifetimes of heterogeneous tryptophan residues in globular proteins between 293 and 77 K. *Photochem Photobiol* **29**:261–265.
128. Domanus J, Strambini GB, Galley WC. 1980. Heterogeneity in the thermally-induced quenching of the phosphorescence of multi-tryptophan proteins. *Photochem Photobiol* **31**:15–21.
129. Barboy N, Feitelson J. 1985. Quenching of tryptophan phosphorescence in alcohol dehydrogenase from horse liver and its temperature dependence. *Photochem Photobiol* **41**(1):9–13.
130. Saviotti ML, Galley WC. 1974. Room temperature phosphorescence and the dynamic aspects of protein structure. *Proc Natl Acad Sci USA* **71**(10):4154–4158.
131. Strambini GB. 1983. Singular oxygen effects on the room-temperature phosphorescence of alcohol dehydrogenase from horse liver. *Biophys J* **43**:127–130.
132. Papp S, Vanderkooi JM. 1989. Tryptophan phosphorescence at room temperature as a tool to study protein structure and dynamics. *Photochem Photobiol* **49**:775–784.
133. Vanderkooi JM, Berger JW. 1989. Excited triplet states used to study biological macromolecules at room temperature. *Biochim Biophys Acta* **976**:1–27.
134. Schauerte JA, Steel DG, Gafni A. 1997. Time-resolved room temperature tryptophan phosphorescence in proteins. *Methods Enzymol* **278**:49–71.
135. Strambini GB, Cioni P. 1999. Pressure-temperature effects on oxygen quenching of protein phosphorescence. *J Am Chem Soc* **121**: 8337–8344.
136. Bodis E, Strambini GB, Gonnelli M, Malnasi-Csizmadia A, Somogyi B. 2004. Characterization of f-actin tryptophan phosphorescence in the presence and absence of tryptophan-free myosin motor domain. *Biophys J* **87**:1146–1154.
137. Mazhul VM, Zaitseva EM, Shavlovsky MM, Stepanenko OV, Kuznetsova IM, Turoverov KK. 2003. Monitoring of actin unfolding by room temperature tryptophan phosphorescence. *Biochemistry* **42**: 13551–13557.
138. Gershenson A, Schauerte JA, Giver L, Arnold FH. 2000. Tryptophan phosphorescence study of enzyme flexibility and unfolding in laboratory-evolved thermostable esterases. *Biochemistry* **39**:4658–4665.
139. Cioni P. 2000. Oxygen and acrylamide quenching of protein phosphorescence: correlation and protein dynamics. *Biophys Chem* **87**: 15–24.
140. Gonnelli M, Strambini GB. 1997. Time-resolved protein phosphorescence in the stopped-flow: denaturation of horse liver alcohol dehydrogenase by urea and guanidine hydrochloride. *Biochemistry* **36**: 16212–16220.
141. Vanderkooi JM, Calhoun DB, Englander SW. 1987. On the prevalence of room-temperature protein phosphorescence. *Science* **230**: 568–569
142. Strambini GB, Gonnelli M. 1990. Tryptophan luminescence from liver alcohol dehydrogenase in its complexes with coenzyme: a comparative study of protein conformation in solution. *Biochemistry* **29**: 196–203.
143. Strambini GB, Gabellieri E. 1989. Phosphorescence properties and protein structure surrounding tryptophan residues in yeast, pig, and rabbit glyceraldehyde-3-phosphate dehydrogenase. *Biochemistry* **28**: 160–166.
144. Strambini GB, Cioni P, Cook PF. 1996. Tryptophan luminescence as a probe of enzyme conformation along the O-acetylserine sulfhydrylase reaction pathway. *Biochemistry* **35**:8392–8400.

145. Burns LE, Maki AH, Spotts R, Matthews KS. 1993. Characterization of the two tryptophan residues of the lactose repressor from *Escherichia coli* by phosphorescence and optical detection of magnetic resonance. *Biochemistry* **32**:12821–12829.
146. Strambini GB, Gabellieri E, Gonnelli M, Rahuel-Clermont S, Branlant G. 1998. Tyrosine quenching of tryptophan phosphorescence in glyceraldehyde-3-phosphate dehydrogenase from *Bacillus stearothermophilus*. *Biophys J* **74**:3165–3172.
147. Brochon JC, Wahl Ph, Charlier M, Maurizot JC, Helene C. 1977. Time-resolved spectroscopy of the tryptophyl fluorescence of the *E. coli* lac repressor. *Biochem Biophys Res Commun* **79**:1261–1271.
148. Eisenberg D, Crothers D. 1979. *Physical chemistry with applications to the life sciences*. Addison-Wesley, Reading, MA. (See page 240.)
149. MacKerell AD, Rigler R, Nilsson L, Hahn U, Saenger W. 1987. A time-resolved fluorescence, energetic and molecular dynamics study of ribonuclease T_1. *Biophys Chem* **26**:247–261.

PROBLEMS

P17.1. *Rotational Diffusion of Proteins*: Use the data in Table 17.7 to calculate the activation energy for rotational diffusion of RNase T_1 in aqueous solution. Also, predict the steady-state anisotropy of RNase T_1 at each temperature from the time-resolved data.

P.17.2. *Rotational Freedom of Tryptophan Residues in Proteins*: Use the data in Table 17.4 to calculate the cone angle for tryptophan motion, independent of overall rotational diffusion. Assume the fundamental anisotropy is 0.31. Perform the calculation for RNase T_1, staph. nuclease, monellin, melittin monomer, and melittin tetramer.

P.17.3. *Apparent Time-Zero Anisotropies of Proteins*: The time-zero anisotropies from RNase T_1 are different in Tables 17.4 and 17.7. Describe possible reasons for these differences.

P.17.4. *Calculation of Decay Associated Spectra*: The *lac* repressor from *E. coli* is a tetrameric protein with two tryptophan residues per subunit. The intensity decays and emission spectra are shown in Figure 17.48, and the intensity decays are given in Table 17.8.

A. Explain the intensity decays (Figure 17.48, left) in terms of the mean lifetime at each wavelength.

B. Calculate the decay-associated spectra and interpret the results.

Table 17.7. Rotational Correlation Times (λ), and Time-Zero Anisotropies, $r(0)$, for RNase T_1 at Various Temperatures[a]

T (°C)	η/T (x10⁻³ kg) (m⁻¹ s⁻¹ K⁻¹)	τ (ns)	r_0	λ (ns)
–1.5	6.63	4.50	0.183 ± 0.007	20.9 ± 1.1
1.5	6.18	4.45	0.176 ± 0.003	15.6 ± 0.8
15.4	3.92	4.19	0.184 ± 0.004	9.6 ± 0.6
29.9	2.63	3.83	0.187 ± 0.004	6.0 ± 0.4
44.4	1.89	3.33	0.197 ± 0.003	3.7 ± 0.2

[a]Also listed are the calculated values of η/*T*, where η is the solution viscosity. From [54].

Table 17.8. Intensity Decays of the *E. coli* lac Repressor[a]

λ_{em} (nm)	τ_1 = 3.8 ns α_1 (λ)	τ_2 = 9.8 ns α_2 (λ)
315	0.72	0.28
320	0.64	0.36
330	0.48	0.52
340	0.35	0.65
350	0.28	0.72
360	0.18	0.82
370	0.08	0.92
380	–	1.00

[a]From [147].

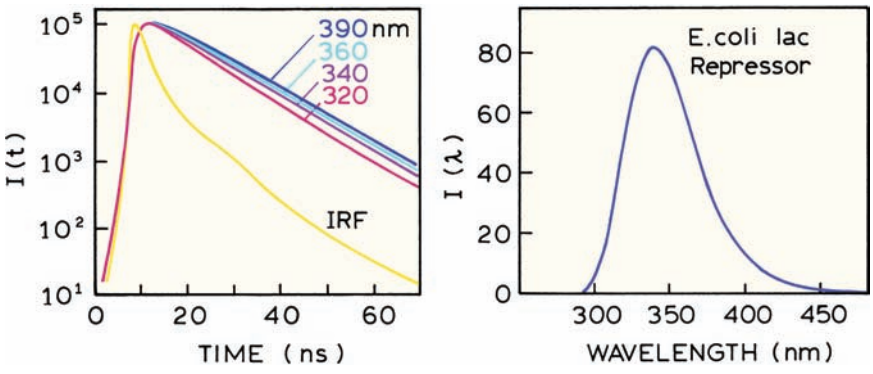

Figure 17.48. Intensity decays at the indicated emission wavelength (left) and emission spectrum (right) of the *E. coli lac* repressor. IRF is the instrument response function. Revised from [147].

C. How could you confirm this assignment of the DAS to each tryptophan residue?

P17.5. *Calculation of a Tryptophan-to-Heme Distance*: Figure 17.36 shows the crystal structure of soybean peroxidase. The dominant component in the tryptophan intensity decay is 35 ps, which accounts for 97% of the emission. Assume the other components are due to impurities or apoprotein, so that the transfer efficiency is up to 97%. Calculate the tryptophan-to-heme distance using the overlap intergral of $J(\lambda) = 9.1 \times 10^{-14}$ M^{-1} cm^3 or the Förster distance of 35.1 Å for $\kappa^2 = 2/3$. The crystal structure indicates $\kappa^2 = 2$. Assume a quantum yield of 0.1 in the absence of energy transfer and a refractive index of 1.3.